Supporting Information

Development of the fluorescent biosensor *h*calmodulin (*h*CaM)L39C-*monobromobimane*(*mBBr*) /V91C-*mBBr*, a novel tool for discovering new calmodulin inhibitors and detecting calcium

Martín González-Andrade,[a] José Rivera-Chávez,[a] Alejandro Sosa-Peinado,[b] Mario Figueroa,[a] Rogelio Rodríguez-Sotres[a] and Rachel Mata[a*]

[a]School of Chemistry, Universidad Nacional Autónoma de México, México DF 04510, México.
[b]School of Medicine, Universidad Nacional Autónoma de México, México DF 04510, México.

*Corresponding author. Dra. Rachel Mata, Facultad de Química, Universidad Nacional Autónoma de México, México DF 04510. Tel.: +525 55 622 5289; fax: +525 55 622 5329.

E-mail address: rachel@servidor.unam.mx

Table of Contents **Page**

1. Characterization physical and spectroscopic parameters of xanthones **1**, **3-5**, **7** and, **8**……..…….....S3
2. Figure S1. ^{1}H NMR spectrum of shamixanthone in $CDCl_3$……..…S6
3. Figure S2. ^{13}C NMR spectrum of shamixanthone in $CDCl_3$……....S7
4. Figure S3. ^{1}H NMR spectrum of tajixanthone in CD_2Cl_2……....S8
5. Figure S4. ^{13}C NMR spectrum of tajixanthone in CD_2Cl_2……...S9
6. Figure S5. ^{1}H NMR spectrum of 14-methoxytajixanthone in $CDCl_3$……....S10
7. Figure S6. ^{13}C NMR spectrum of 14-methoxytajixanthone in $CDCl_3$……....S11
8. Figure S7. ^{1}H NMR spectrum of tajixanthone hydrate in $CDCl_3$……S12
9. Figure S8. ^{13}C NMR spectrum of tajixanthone hydrate in $CDCl_3$……..…...S13
10. Figure S9. ^{1}H NMR spectrum of 15-acetyl tajixanthone hydrate in $CDCl_3$……..S14
11. Figure S10. ^{13}C NMR spectrum of 15-acetyl tajixanthone hydrate in $CDCl_3$…...S15
12. Figure S11. ^{1}H NMR spectrum of 16-chlorotajixanthone in $CDCl_3$……...S16
13. Figure S12. ^{13}C NMR spectrum of 16-chlorotajixanthone in $CDCl_3$…...…….S17
14. Figure S13. ^{1}H NMR spectrum of emericellin in $CDCl_3$……..…….....S18
15. Figure S14. ^{13}C NMR spectrum of emericellin in $CDCl_3$……...……S19
16. Figure S15. ^{1}H NMR spectrum of variecoxanthone A acetate in $CDCl_3$……....S20
17. Figure S16. ^{13}C NMR spectrum of variecoxanthone A acetate in $CDCl_3$…….....S21
18. Figure S17. Fluorescence spectra changes of the titration of *h*CaM L39C-*mBBr*/V91C-*mBBr* with shamixanthone (**1**)…….S22
19. Figure S18. Fluorescence spectra changes of the titration of *h*CaM L39C-*mBBr*/V91C-*mBBr* with tajixanthone (**2**)…….S23
20. Figure S19. Fluorescence spectra changes of the titration of *h*CaM L39C-*mBBr*/V91C-*mBBr* with 14-methoxytajixanthone (**3**)……..S24
21. Figure S20. Fluorescence spectra changes of the titration of *h*CaM L39C-*mBBr*/V91C-*mBBr* with tajixanthone hydrate (**4**)……S25
22. Figure S21. Fluorescence spectra changes of the titration of *h*CaM L39C-*mBBr*/V91C-*mBBr* with 15-acetyl tajixanthone hydrate (**5**)……S26
23. Figure S22. Fluorescence spectra changes of the titration of *h*CaM L39C-*mBBr*/V91C-*mBBr* with 16-chlorotajixanthone (**6**)…….....S27
24. Figure S23. Fluorescence spectra changes of the titration of *h*CaM L39C-*mBBr*/V91C-*mBBr* with emericelline (**7**)…….S28
25. Figure S24. Fluorescence spectra changes of the titration of *h*CaM L39C-*mBBr*/V91C-*mBBr* with variecoxanthone A acetate (**8**)……...S29
26. Figure S25. Structural model of Ca^{+2}-CaM-**1** complex…….…….....S30
27. Figure S26. Structural model of Ca^{+2}-CaM-**3** complex…….....S31
28. Figure S27. Structural model of Ca^{+2}-CaM-**4** complex…….....S32
29. Figure S28. Structural model of Ca^{+2}-CaM-**5** complex…….....S33
30. Figure S29. Structural model of Ca^{+2}-CaM-**7** complex…….……S34
31. Figure S30. Structural model of Ca^{+2}-CaM-**8** complex…….……S35

Characterization physical and spectroscopic parameters of xanthones 1, 3-5, 7 and, 8.

Shamixanthone (1): Yellow needles, mp 141–143 °C; $[\alpha]_D^{23}$ +34.1 (*c* 0.1, $CHCl_3$); UV λ_{max} ($CHCl_3$/nm (log ε) 395 (3.50), 2.90 (346), 299 (3.77), 293 (3.76), 276 (4.24), 250 (4.05), 244 (4.07).^{1}H NMR (300 MHz, $CDCl_3$) δ 12.60 (s, 1H), 7.44 (d, J = 8.4 Hz, 1H), 7.30 (s, 1H), 6.74 (d, J = 8.4 Hz, 1H), 5.41 (s, 1H), 5.31 (dd, J = 7.2, 7.6 Hz, 1H), 5.09 (s, 1H), 4.80 (s, 1H), 4.58 (s, 1H), 4.43 (dd, J = 2.8, 11.2 Hz, 1H), 4.34 (dd, J = 2.8, 10.8 Hz, 1H), 3.50 (d, J = 6.0 Hz, 1H), 3.49 (d, J = 5.5 Hz, 1H), 2.73 (s, 1H), 2.36 (s, 3H), 1.85 (s, 3H), 1.79 (s, 3H), 1.75 (s, 3H); ^{13}C NRM (75 MHz, $CDCl_3$) δ 184.5, 152.8, 152.3, 159.7, 149.4, 142.6, 138.4, 136.6, 133.3, 121.7, 120.8, 119.4, 118.9, 116.7, 112.3, 109.8, 109.2, 64.6, 63.2, 44.9, 27.5, 25.8, 22.6, 17.9, 17.5; HRMS-EI $[M]^+$ *m/z* 406.471 (calcd for $C_{25}H_{26}O_5$ 406.479).

Tajixanthone (2): Yellow needles, mp 153–155 °C; IR υ_{max} (film)/cm^{-1} 3468, 3918, 1643, 1603, 1575, 1477, 1244; ^{1}H NMR (300 MHz, $CDCl_3$) δ 12.61 (s, 1H), 7.54 (d, J = 8.4 Hz, 1H), 7.35 (d, J = 0.9 Hz, 1H), 6.76 (d, J = 8.4 Hz, 1H), 5.41 (d, J = 1.8 Hz, 1H), 4.79 (d, J = 0.9 Hz, 1H), 4.57 (d, J = 0.9 Hz, 1H), 4.43 (ddd, J = 1.20, 3.75, 10.95 Hz, 1H), 4.33 (dd, J = 3.0, 10.8 Hz, 1H), 3.0 (dd, J = 4.8, 12.0 Hz, 1H), 2.72 (d, J = 3.0 Hz, 1H), 2.35 (d, J = 0.9 Hz, 3H), 1.87 (s, 3H), 1.84 (sb, 3H), 1.44 (s, 3H), 1.30 (s, 3H); ^{13}C NMR (75 MHz, $CDCl_3$) δ 184.9, 160.8, 152.5, 151.3, 143.4, 142.0, 139.0, 137.5, 121.7, 119.5, 116.1, 115.9, 112.2, 110.2, 110.0, 65.0, 63.6, 58.9, 45.4, 29.0, 24.9, 22.6, 19.2, 17.5; HRMS-EI $[M]^+$ *m/z* 422.470 (calcd for $C_{25}H_{26}O_5$ 422.479). These data are in agreement with those reported by Chexal and coworkers.[17]

14-Methoxytajixanthone (3): Yellow needles, mp 200–201 °C; $[\alpha]_D^{23}$ –38.0 (*c* 0.1, $CHCl_3$); IR υ_{max} (KBr)/cm^{-1} 3450, 3078, 2592, 2887, 1795, 920; UV λ_{max} ($CHCl_3$)/nm (log ε) 395 (3.23), 346 (2.59), 299 (2.48), 290 (3.42), 277 (3.85), 261 (3.74), 254 (3.78), 248 (3.77), 245 (3.77). ^{1}H NMR (300 MHz, $CDCl_3$) δ 12.86 (s, 1H), 7.72 (d, *J* = 8.5 Hz, 1H), 7.23 (d, *J* = 1.0 Hz, 1H), 6.88 (d, *J* = 8.5 Hz, 1H), 5.43 (d, *J* = 2.1 Hz, 1H), 4.94 (sb, 1H), 4.81 (d, *J* = 2.5 Hz, 1H), 4.67 (d, *J* = 8.0 Hz, 1H), 4.60 (d, *J* = 1.0 Hz, 1H), 4.43 (dd, *J* = 3.6, 10.8 Hz, 1H), 4.35 (dd, *J* = 3.0, 10.8 Hz, 1H), 3.40 (s, 3H), 3.18 (d, *J* = 8.0 Hz, 1H), 2.74 (ddd, *J* = 2.1, 3.0, 3.6 Hz, 1H), 2.36 (s, 3H), 1.85 (s, 3H), 1.32 (s, 3H), 1.25 (s, 3H); ^{13}C NRM (75 MHz, $CDCl_3$) δ 184.4, 162.2, 152.7, 151.9, 149.8, 142.5, 138.9, 135.6, 119.1, 119.0, 116.8, 115.9, 112.3 110.9, 109.0, 76.1, 66.7, 64.7, 63.3, 57.8, 56.9, 45.0, 24.7, 22.7, 19.8, 17.5; HRMS-FAB $[M+1]^+$ *m/z* 453.2074 (calcd for $C_{26}H_{28}O_7$ 453.2066).

Tajixanthone hydrate (4): Yellow needles, mp 182–184 °C; $[\alpha]_D^{23}$-74.0 (c 0.1, $CHCl_3$); UV λ_{max} ($CHCl_3$)/nm (log ε) 397 (3.72), 347 (3.14), 299 (3.92), 294 (3.91), 278 (4.42), 261 (4.25), 257 (4.25), 249 (4.21), 244 (4.24); ^{1}H NMR (300 MHz, $CDCl_3$) δ 12.54 (s, 1H), 7.49 (d, *J* = 8.4 Hz, 1H), 7.19 (s, 1H), 6.72 (d, *J* = 8.4 Hz, 1H), 5.34 (s, 1H), 4.98 (d, *J* = 4.0 Hz, 1H), 4.77 (s, 1H), 4.53 (s, 1H), 4.41 (dd, *J* = 2.0, 10.8 Hz, 1H), 4.31 (dd, *J*=2.8, 10.8 Hz, 1H), 3.70 (d, *J*=10.8 Hz, 1H), 3.16 (dd, *J*=10.8, 14.0 Hz, 1H), 2.69 (s, 1H), 2. 63 (dd, *J*=10.8, 14 Hz, 1H), 2.44 (s, 1H), 2.37 (s, 1H), 2.28 (s, 3H), 1.82 (s, 3H), 1.39 (s, 3H), 1.34 (s, H); ^{13}C NRM (75 MHz, $CDCl_3$) δ 184.3, 160.3, 153.1, 151.9, 149.5, 142.5, 138.5, 138.3, 120.8, 119.1, 116.8, 116.3, 112.3, 109.9, 109.2, 77.7, 72.9, 64.5, 63.2, 44.8, 32.0, 26.5, 23.6, 22.6, 17.4; MS-EI $[M]^+$ *m/z* 440.

Emericelline (**7**): Yellow needles, mp 113–115 °C; ^{1}H NMR (300 MHz, $CDCl_3$) δ 12.92 (d, J = 0.3 Hz, 1H), 7.48 (dd, J = 0.4, 8.4 Hz, 1H), 7.28 (d, J = 7.6 Hz, 1H), 6.85 (d, J = 8.4 Hz, 1H), 5.61 (dd, J = 1.5, 7.2 Hz, 1H), 5.34 (dd, J = 1.5, 7.5 Hz, 1H), 5.09 (d, J = 7.8 Hz, 1H), 4.50 (d, J = 8.1 Hz, 1H), 4.45 (d, J = 7.5 Hz, 1H), 3.39 (d, J = 7.2 Hz, 1H), 2.41 (s, 3H), 1.81 (s, 3H), 1.74 (s, 6H), 1.71 (s, 3H); ^{13}C NRM (75 MHz, $CDCl_3$) δ 184.5, 159.9, 152.8, 152.3, 149.4, 142.6, 138.4, 136.6, 133.3, 123.9, 122.1, 119.5, 119.4, 118.8, 118.7, 109.8, 106.2, 71.6, 52.6 ,27.1, 25.8, 25.3, 18.4, 18.2, 17.9; MS-EI $[M]^+$ *m/z* 408.

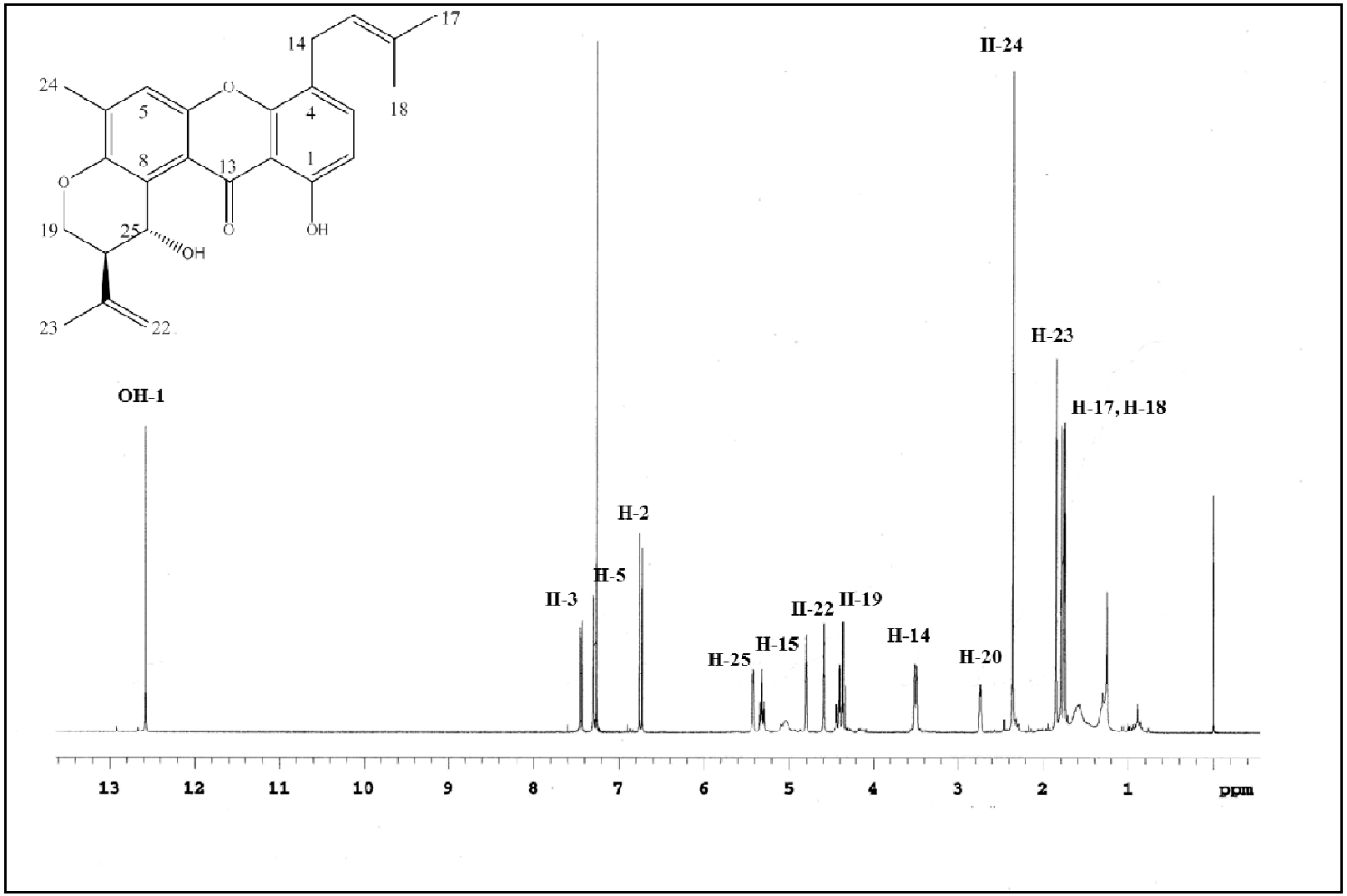

Figure S1. ^{1}H NMR spectrum of shamixanthone in $CDCl_3$.

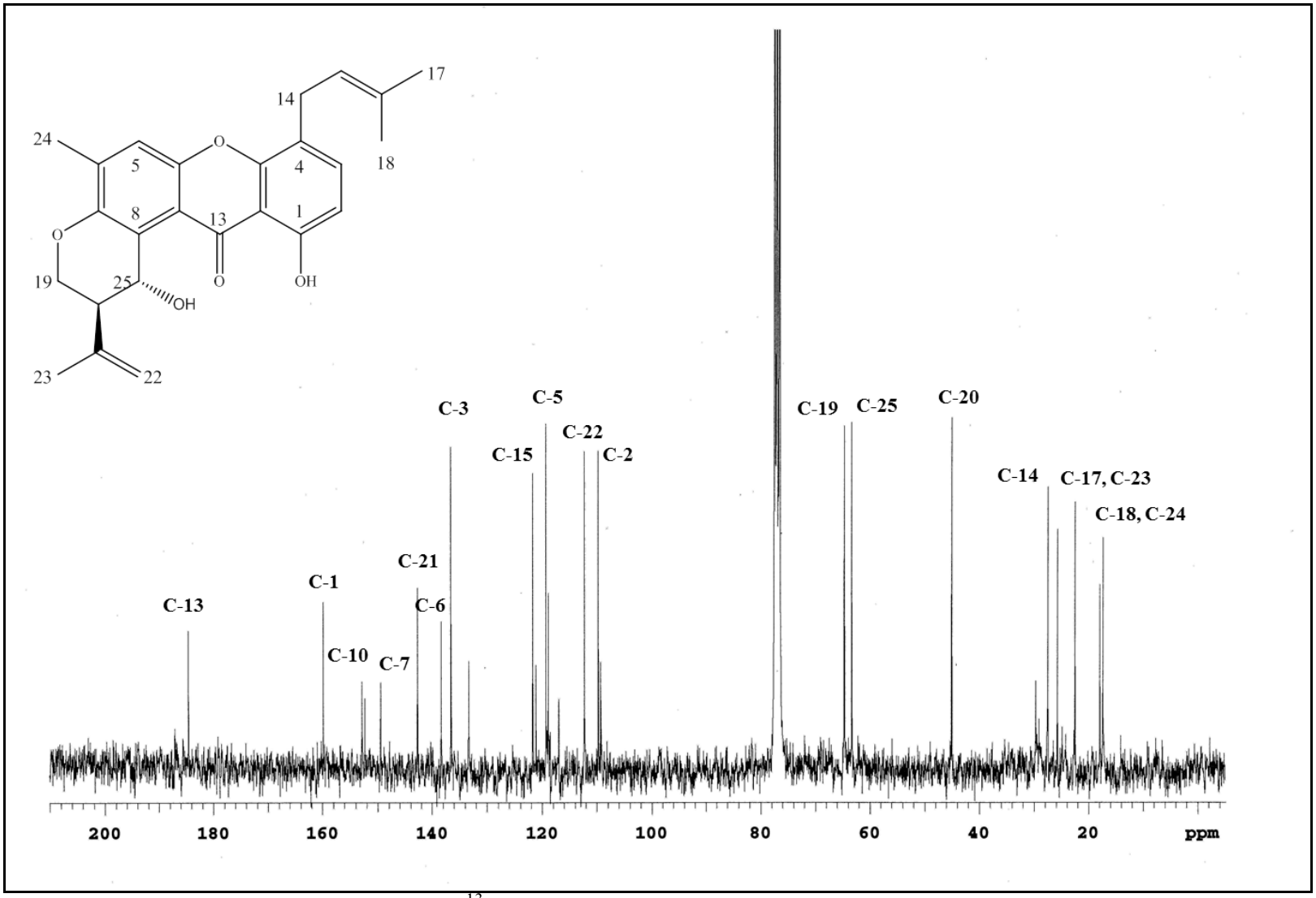

Figure S2. ^{13}C NMR spectrum of shamixanthone in $CDCl_3$.

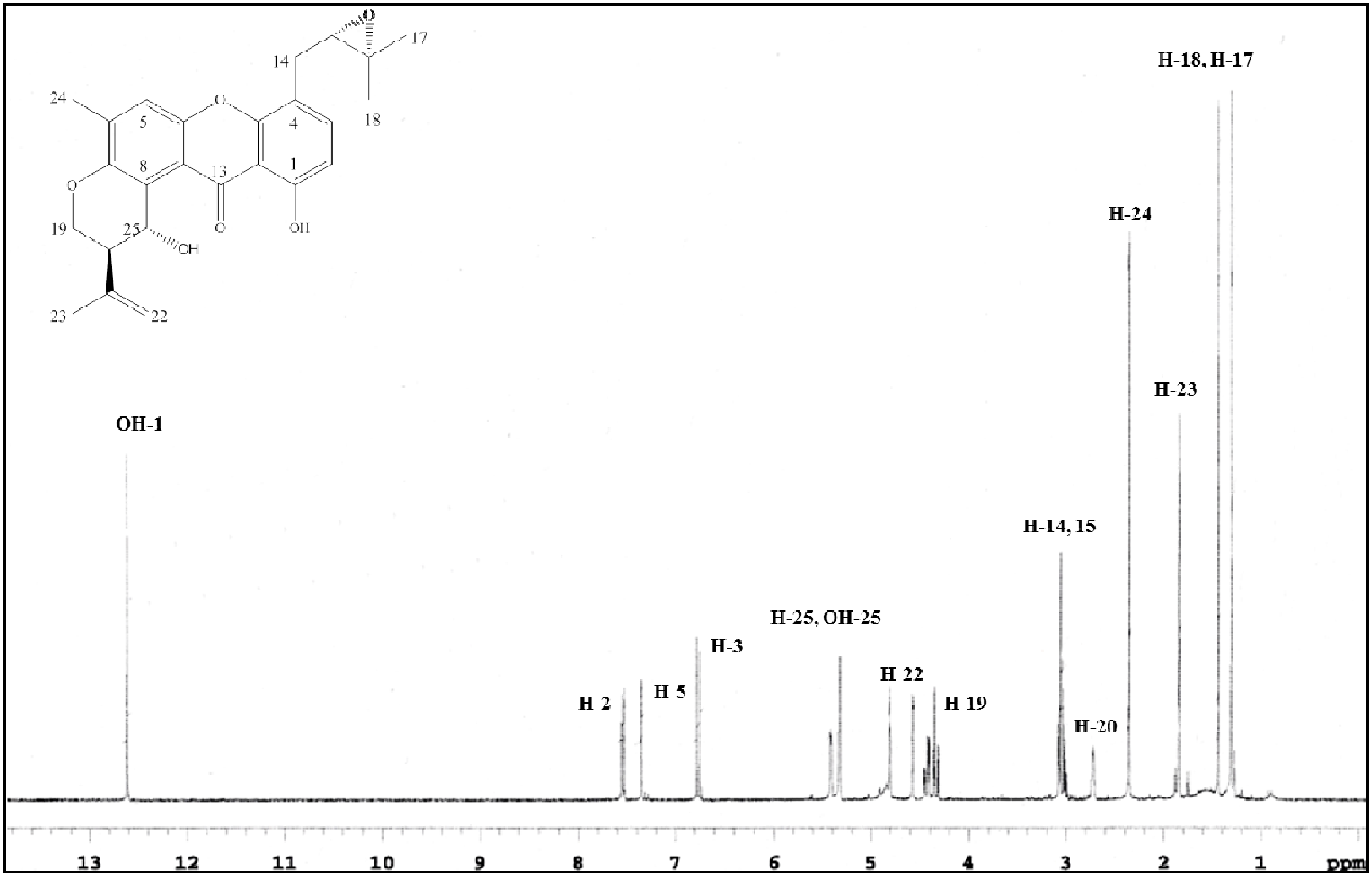

Figure S3. ^{1}H NMR spectrum of tajixanthone in CD_2Cl_2.

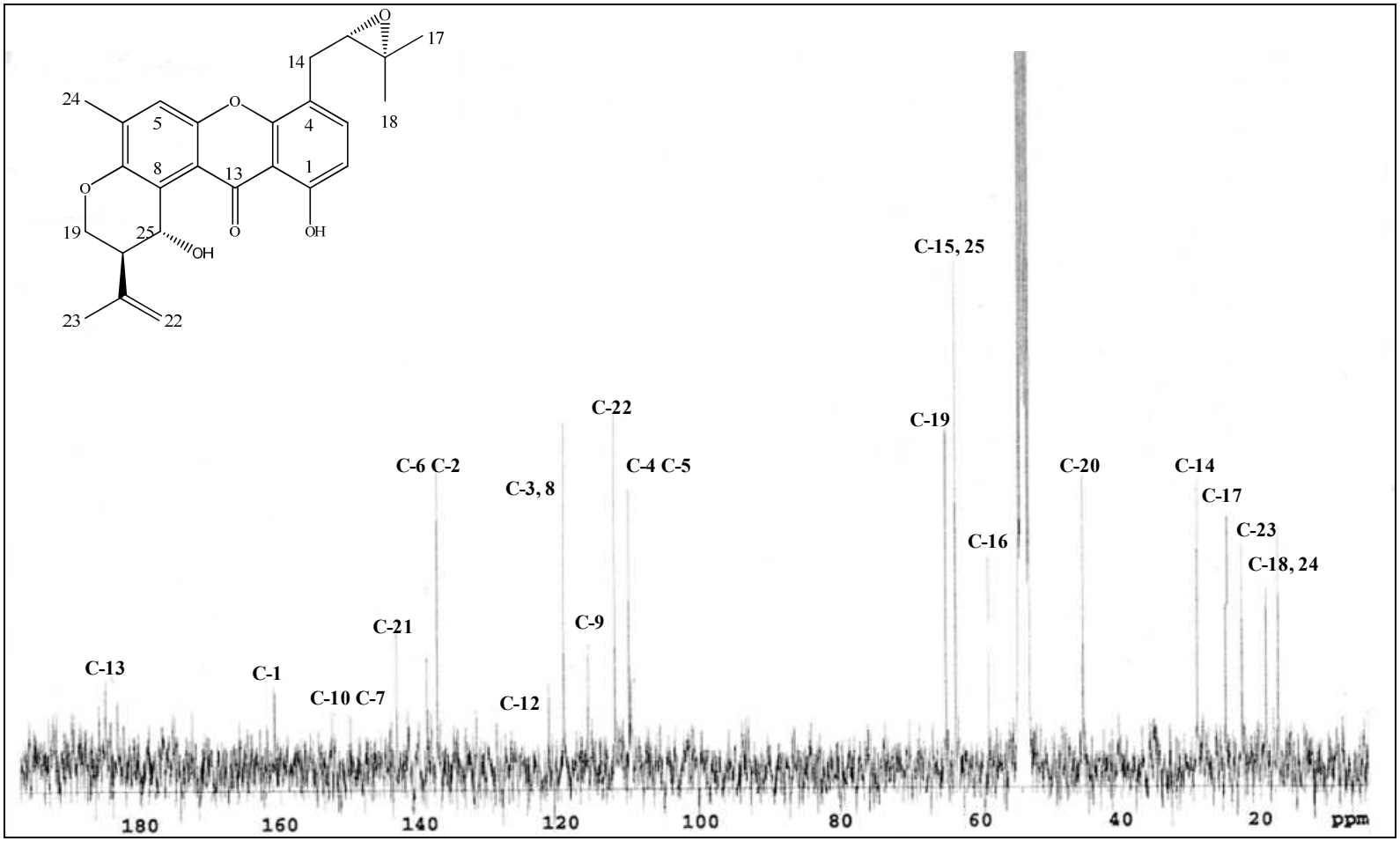

Figure S4. ^{13}C NMR spectrum of tajixanthone in CD_2Cl_2.

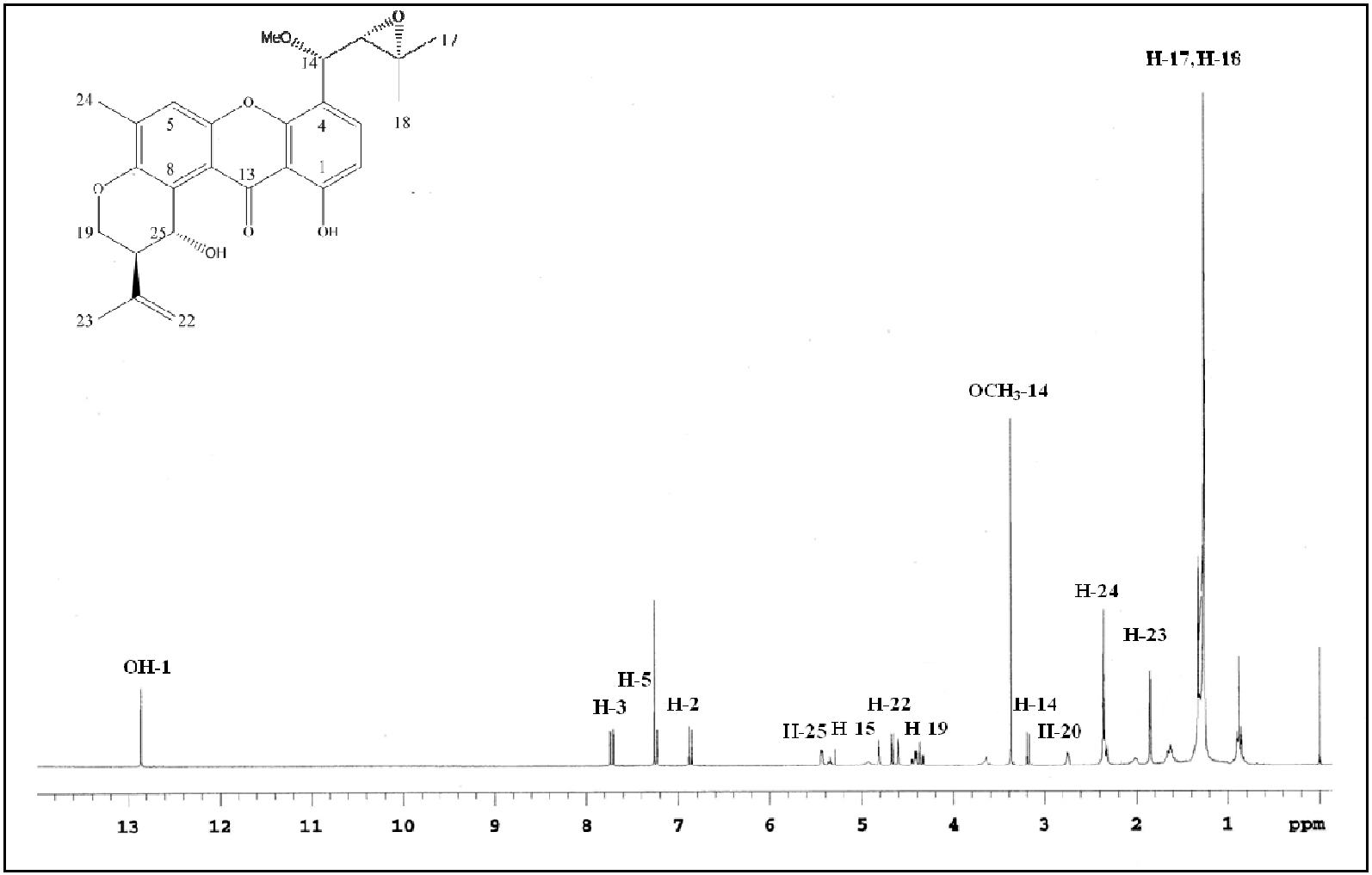

Figure S5. ^{1}H NMR spectrum of 14-methoxytajixanthone in $CDCl_3$.

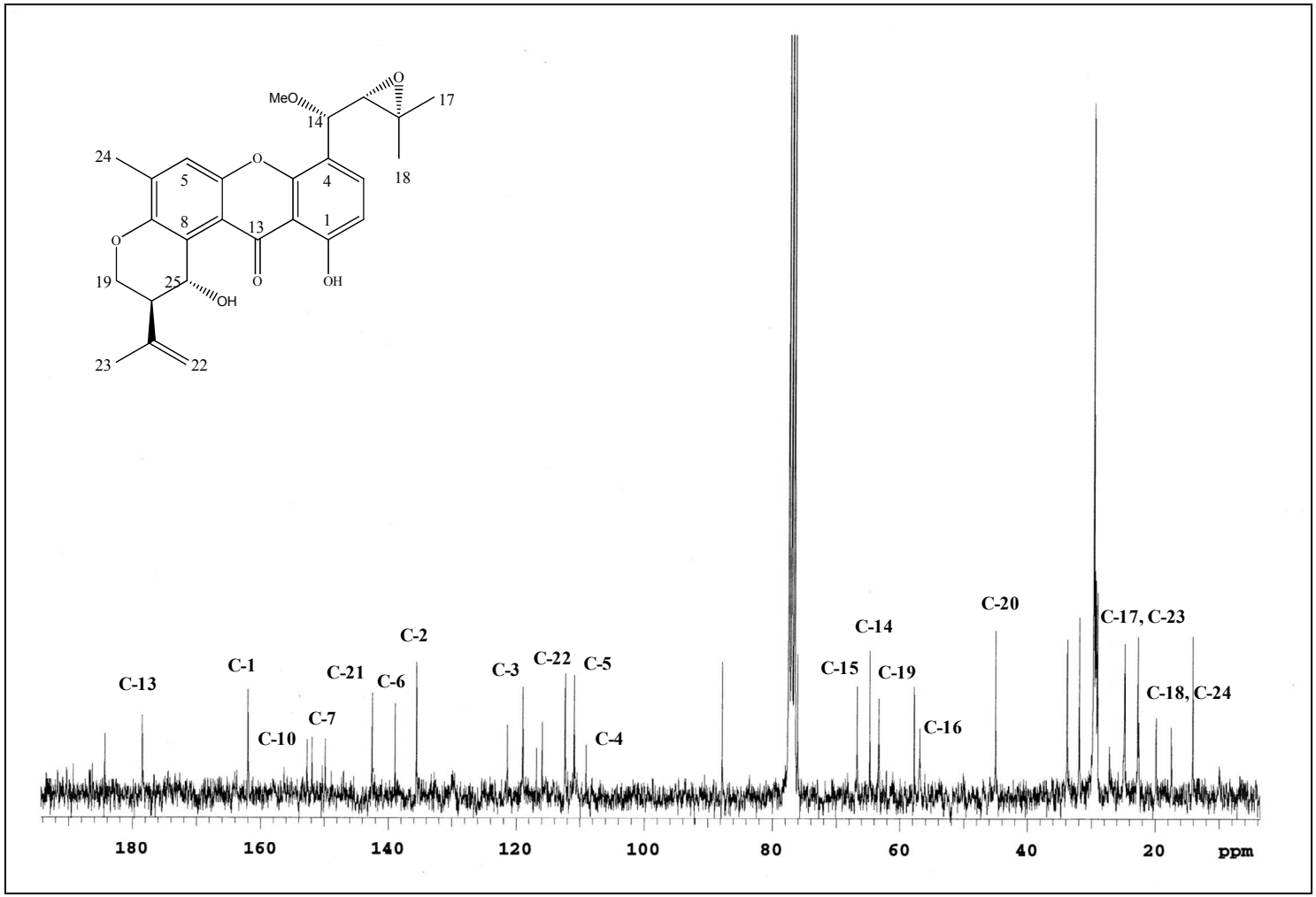

Figure S6. ^{13}C NMR spectrum of 14-methoxytajixanthone in $CDCl_3$.

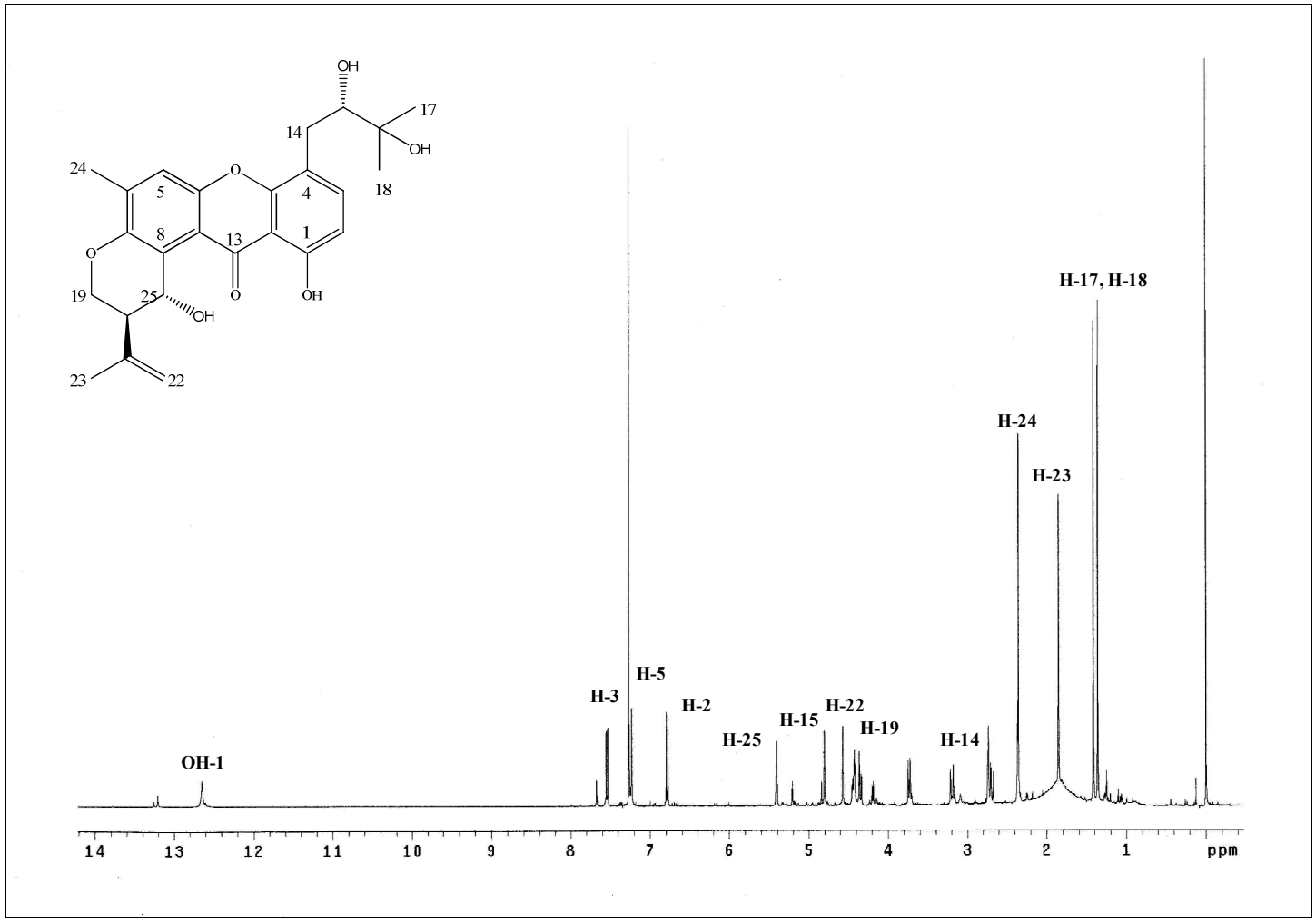

Figure S7. ^{1}H NMR spectrum of tajixanthone hydrate in $CDCl_3$.

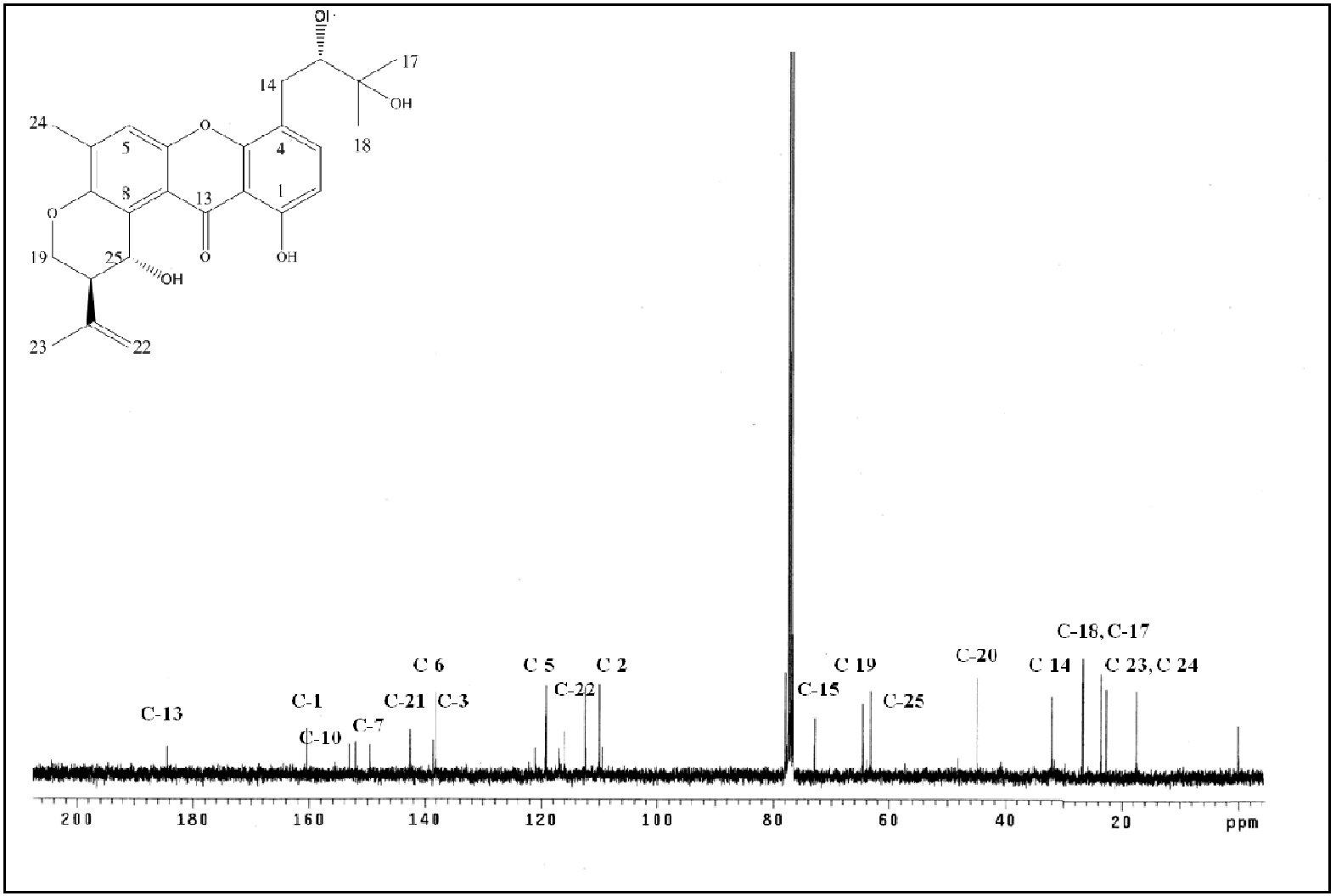

Figure S8. ^{13}C NMR spectrum of tajixanthone hydrate in $CDCl_3$.

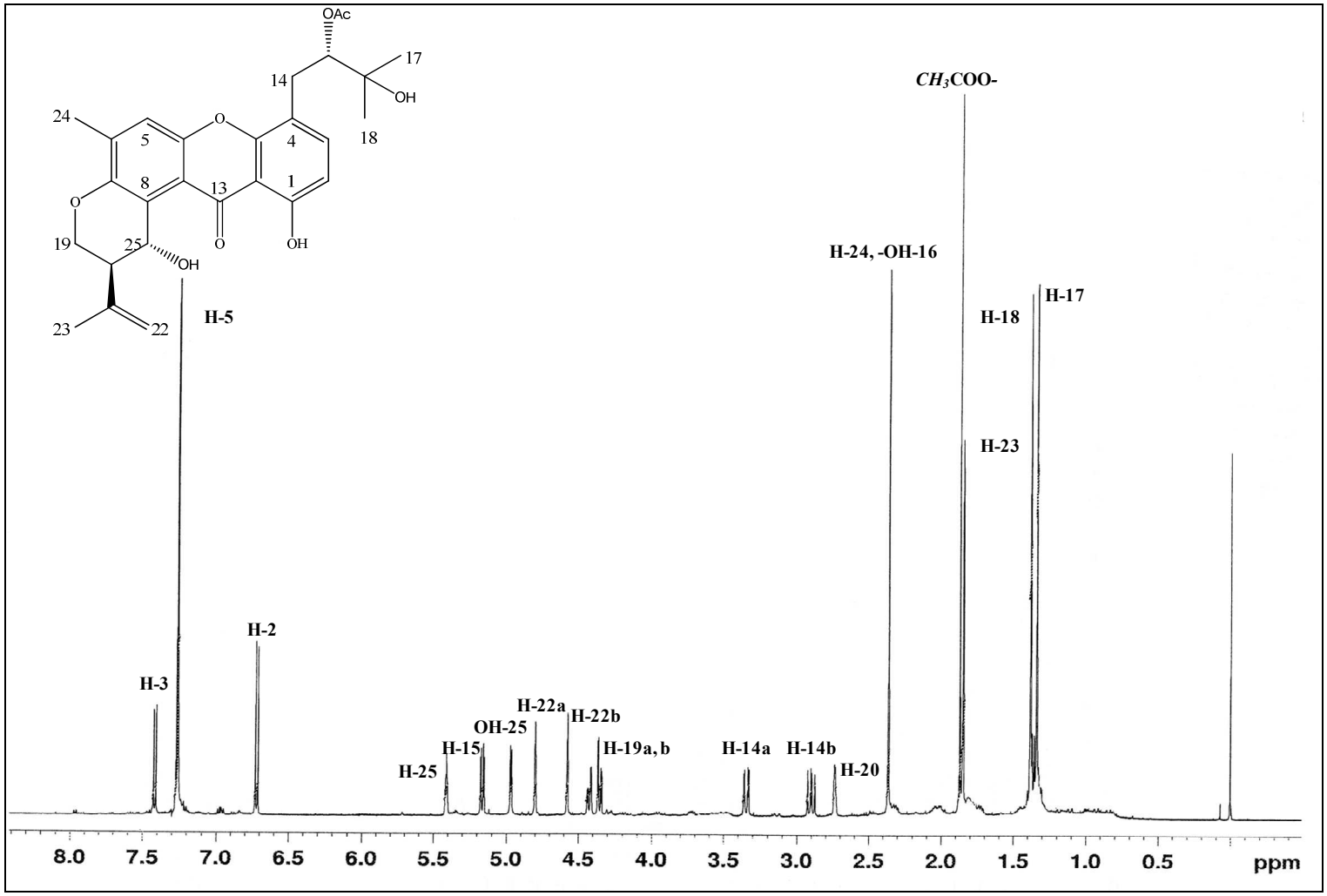

Figure S9. ^{1}H NMR spectrum of 15-acetyl tajixanthone hydrate in $CDCl_3$.

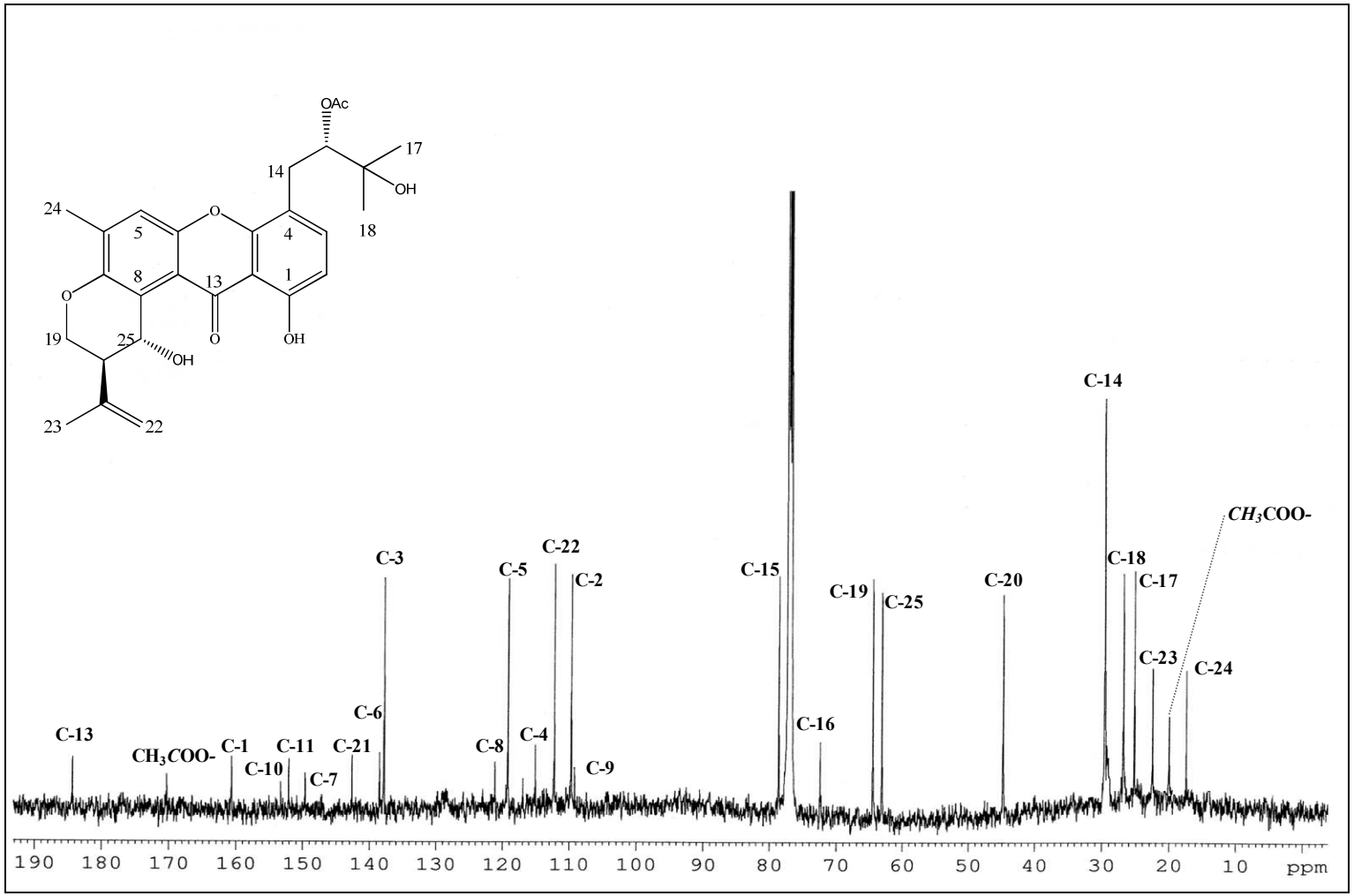

Figure S10. ^{13}C NMR spectrum of 15-acetyl tajixanthone hydrate in $CDCl_3$.

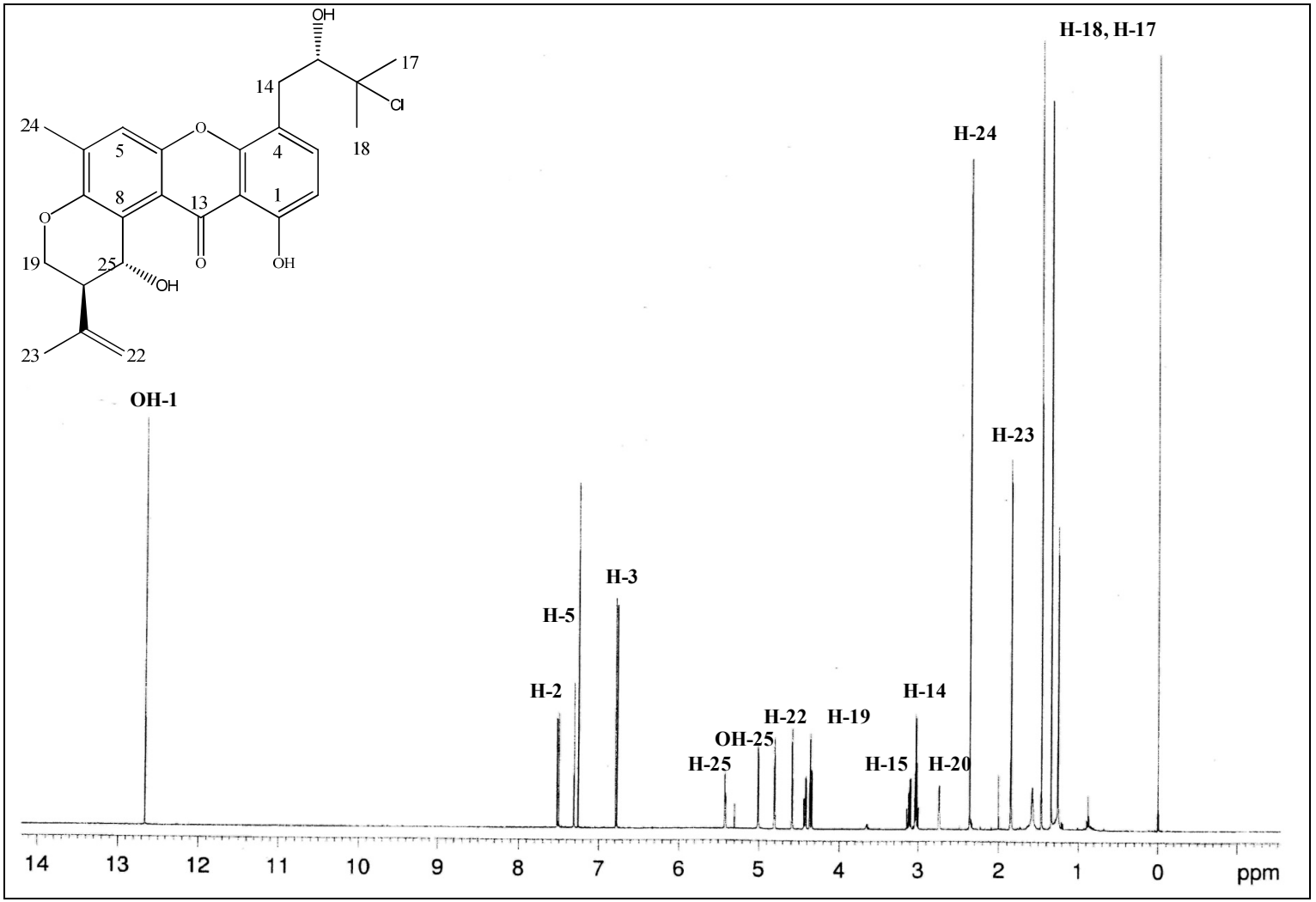

Figure S11. ^{1}H NMR spectrum of 16-chlorotajixanthone in $CDCl_3$.

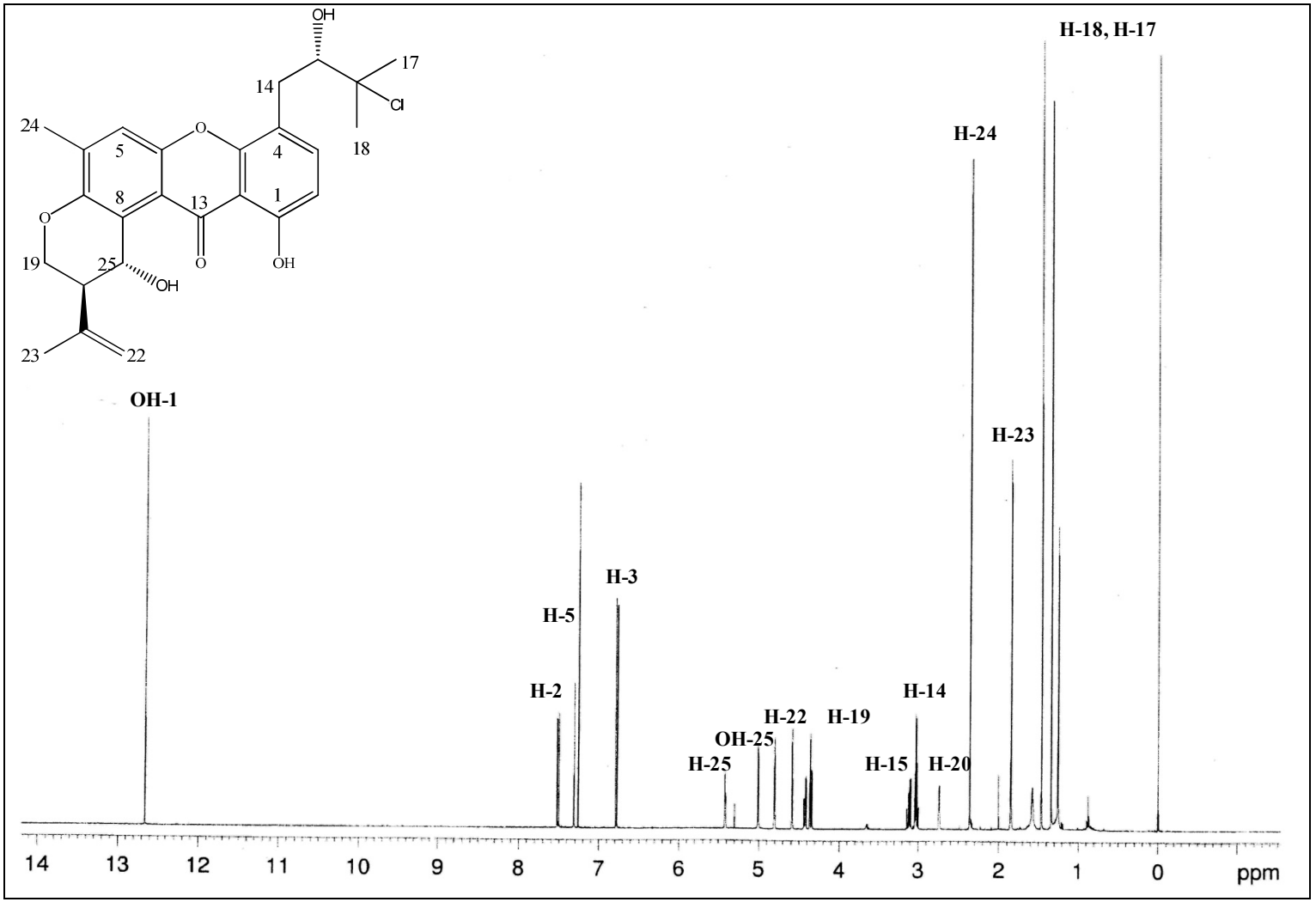

Figure S12. ^{13}C NMR spectrum of 16-chlorotajixanthone in $CDCl_3$.

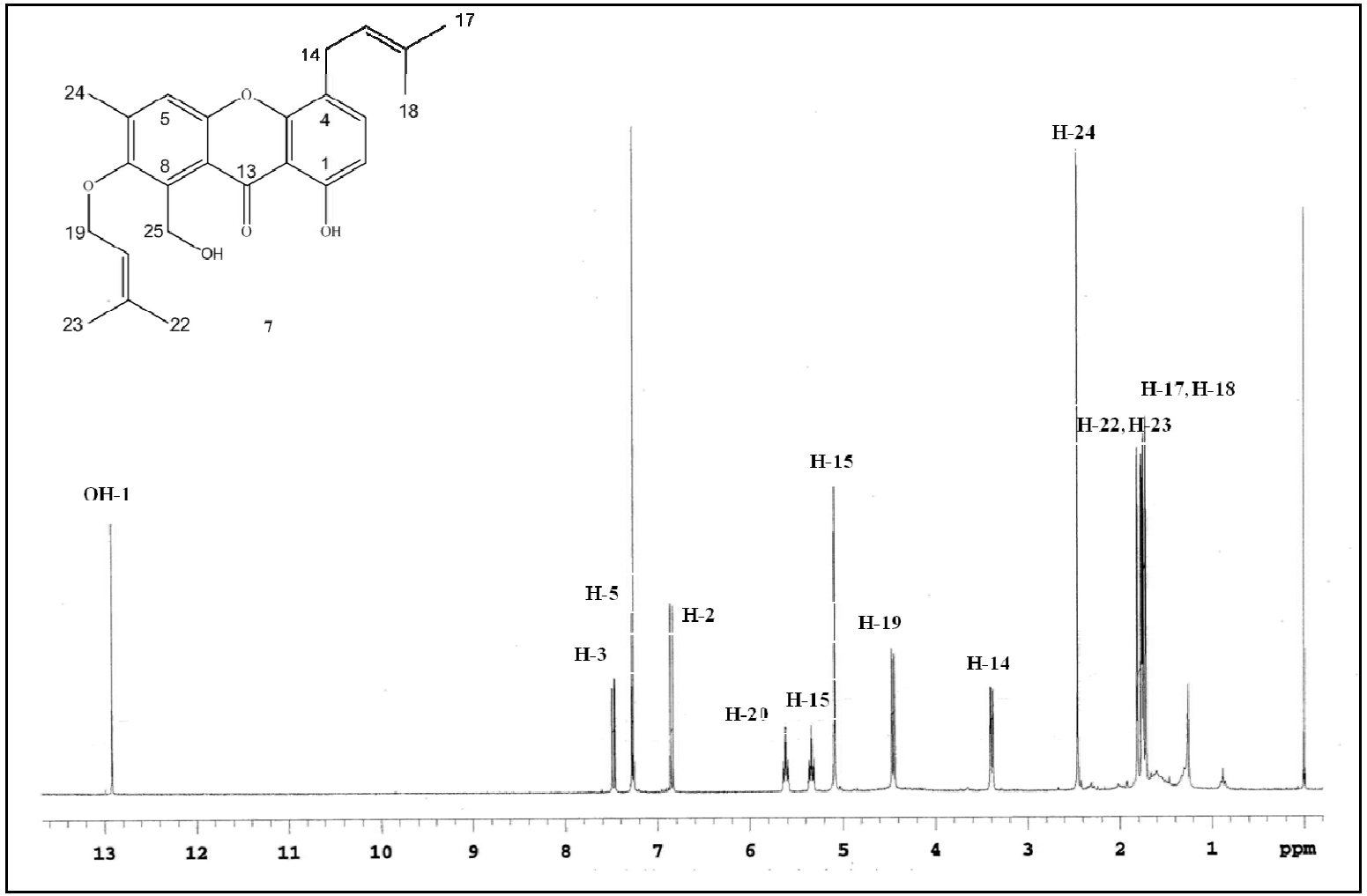

Figure S13. ^{1}H NMR spectrum of emericellin in $CDCl_3$.

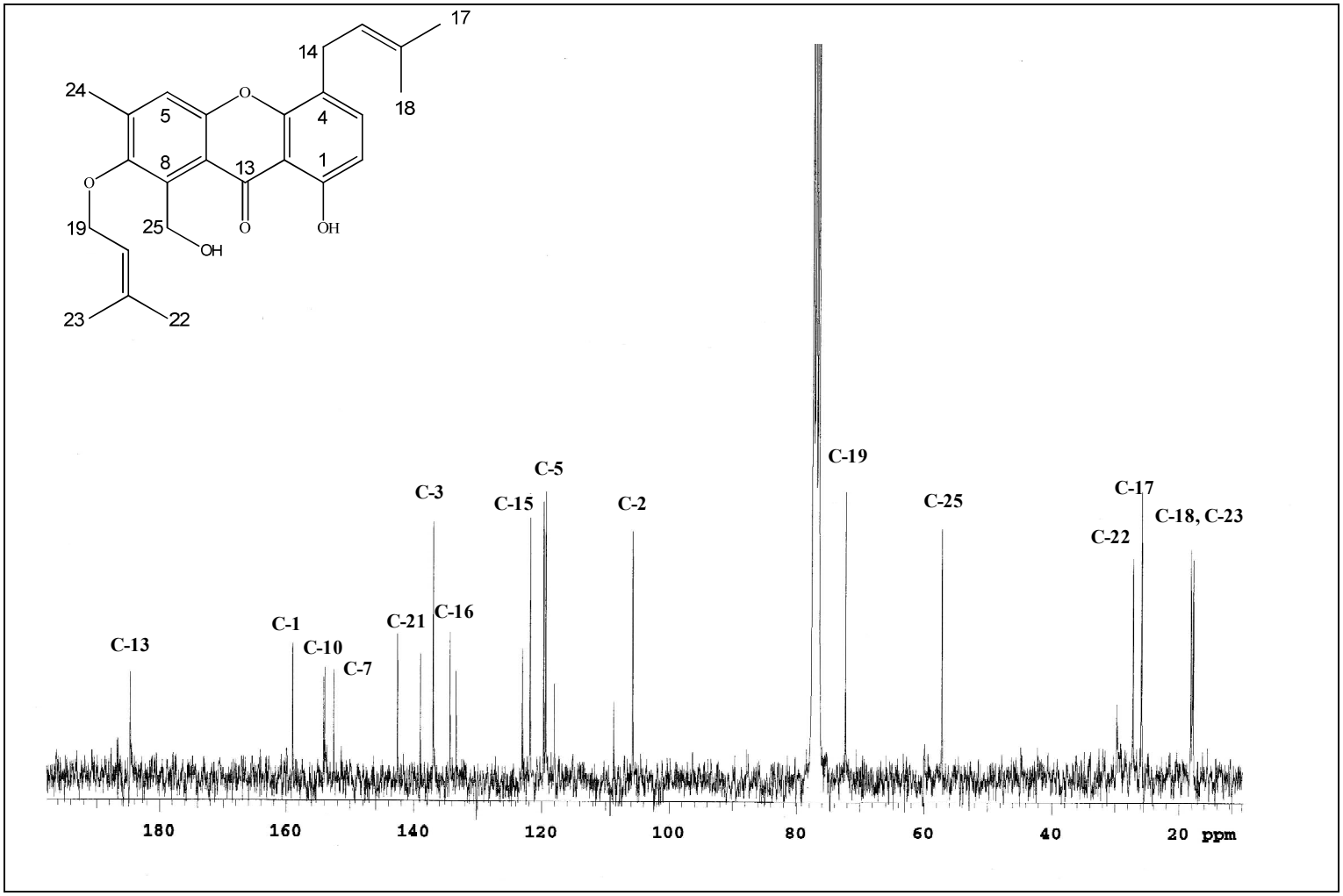

Figure S14. ^{13}C NMR spectrum of emericellin in $CDCl_3$.

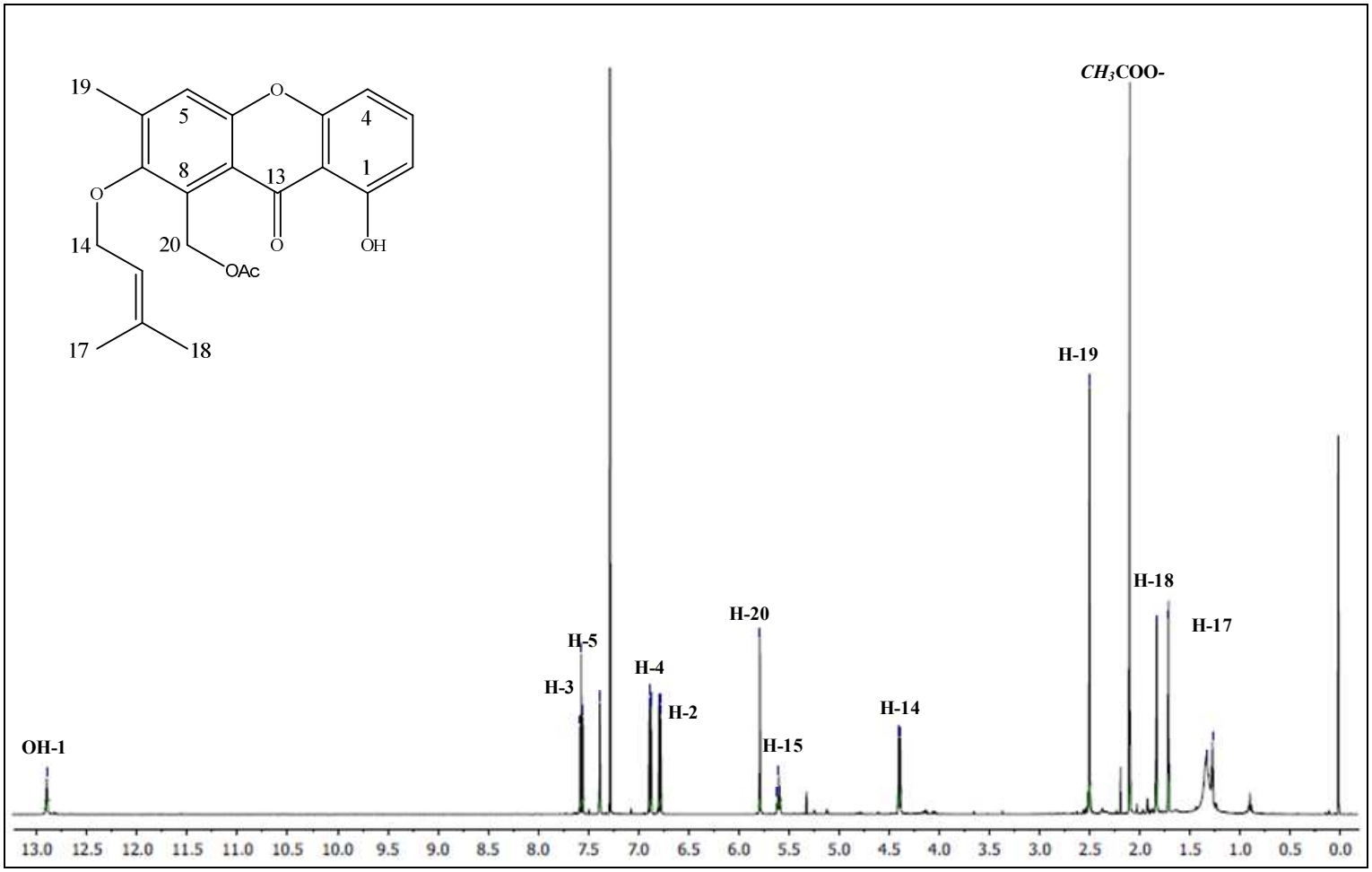

Figure S15. ^{1}H NMR spectrum of variecoxanthone A acetate in $CDCl_3$.

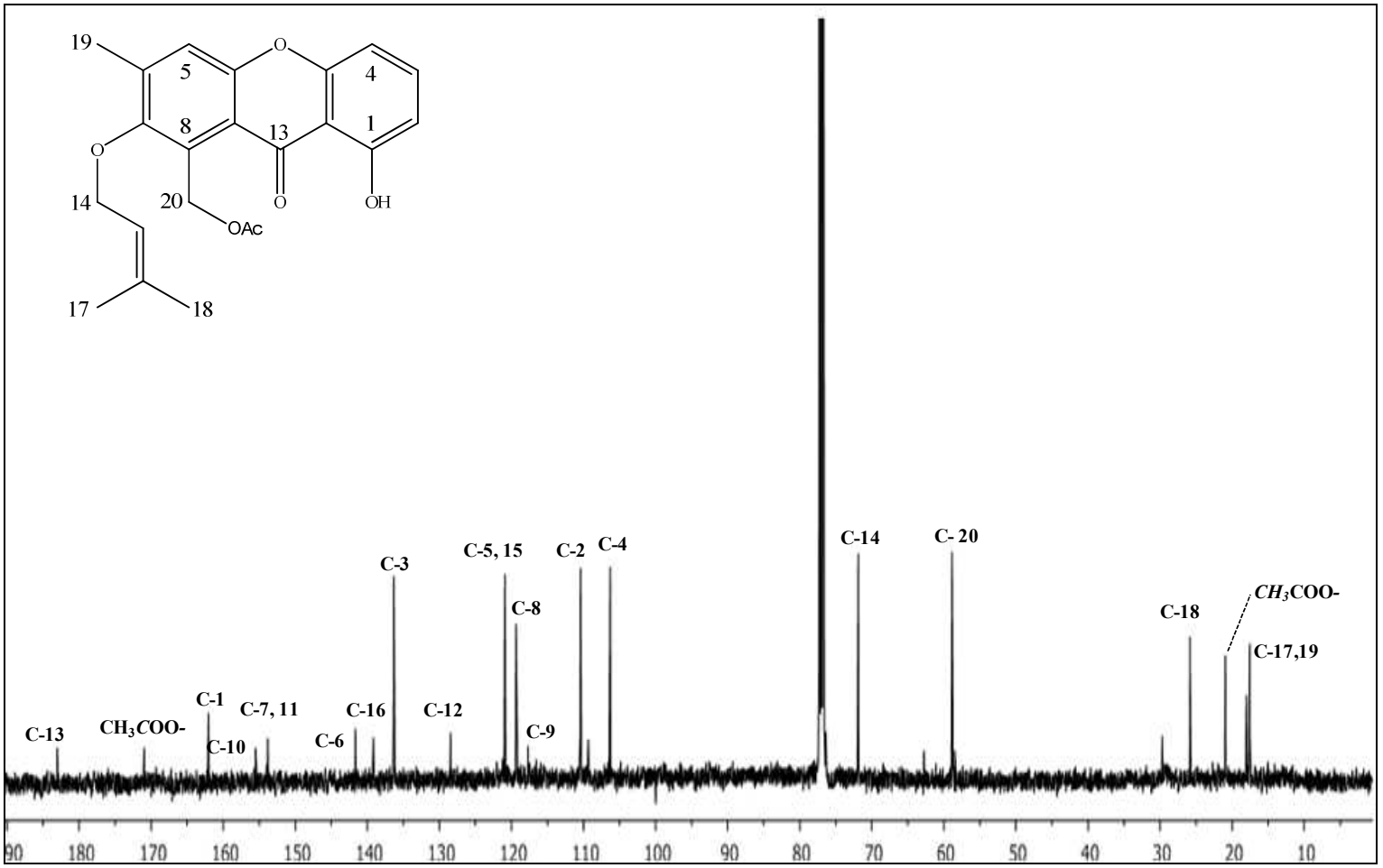

Figure S16. ^{13}C NMR spectrum of variecoxanthone A acetate in $CDCl_3$.

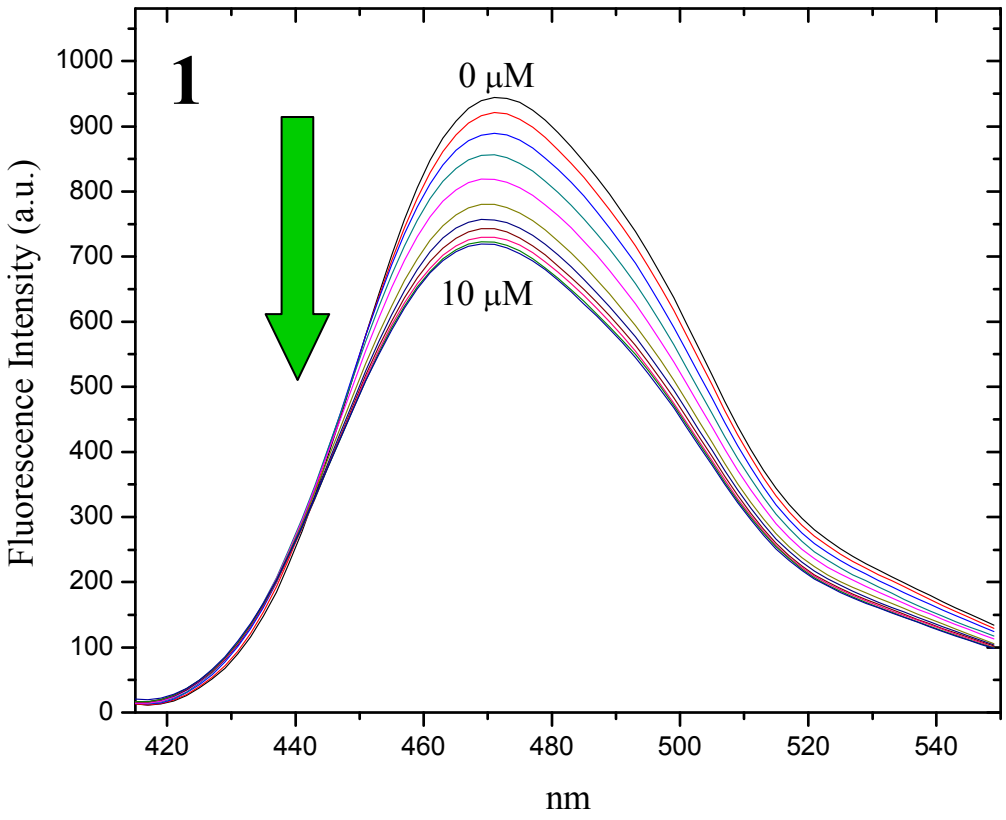

Figure S17. Fluorescence spectra changes of the titration of *h*CaM L39C-*mBBr*/V91C-*mBBr* with shamixanthone (**1**).

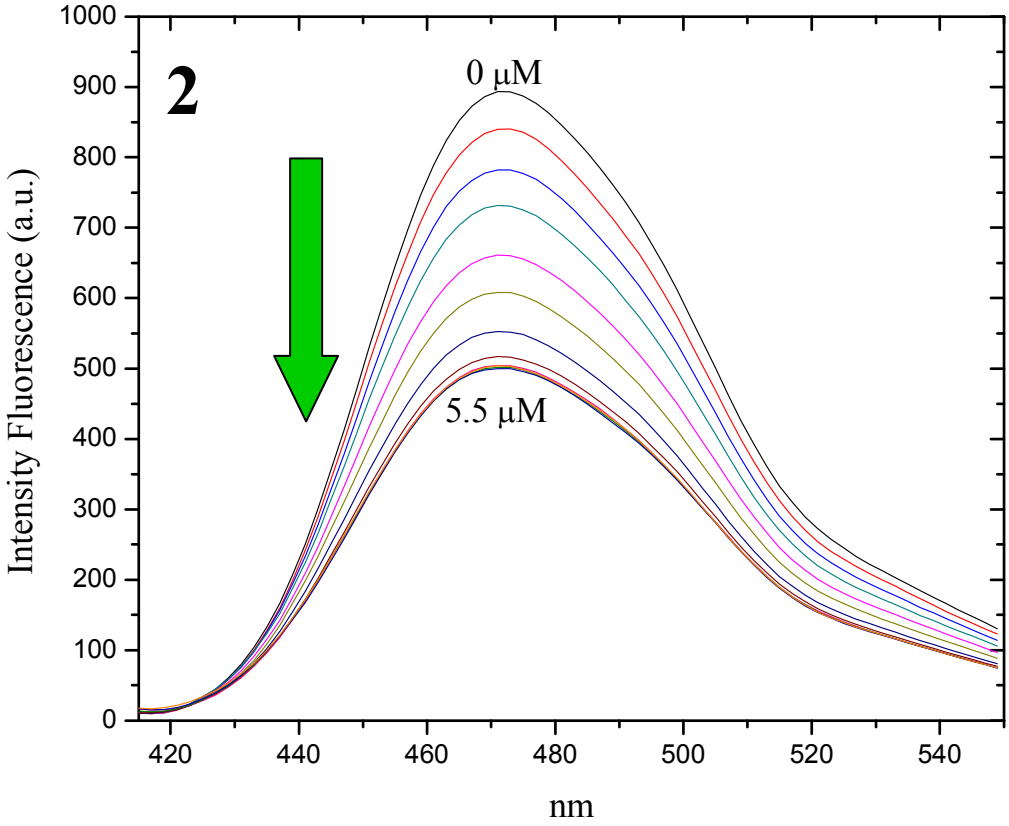

Figure S18. Fluorescence spectra changes of the titration of *h*CaM L39C-*mBBr*/V91C-*mBBr* with tajixanthone (**2**).

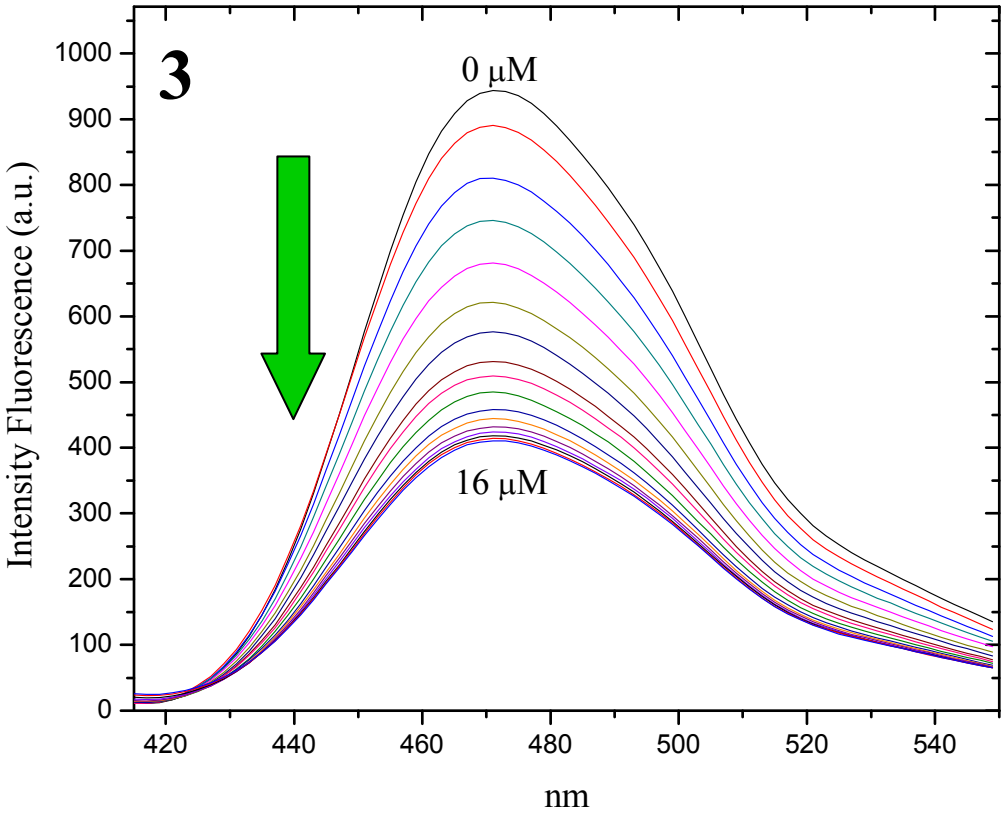

Figure S19. Fluorescence spectra changes of the titration of *h*CaM L39C-*mBBr*/V91C-*mBBr* with 14-methoxytajixanthone (**3**).

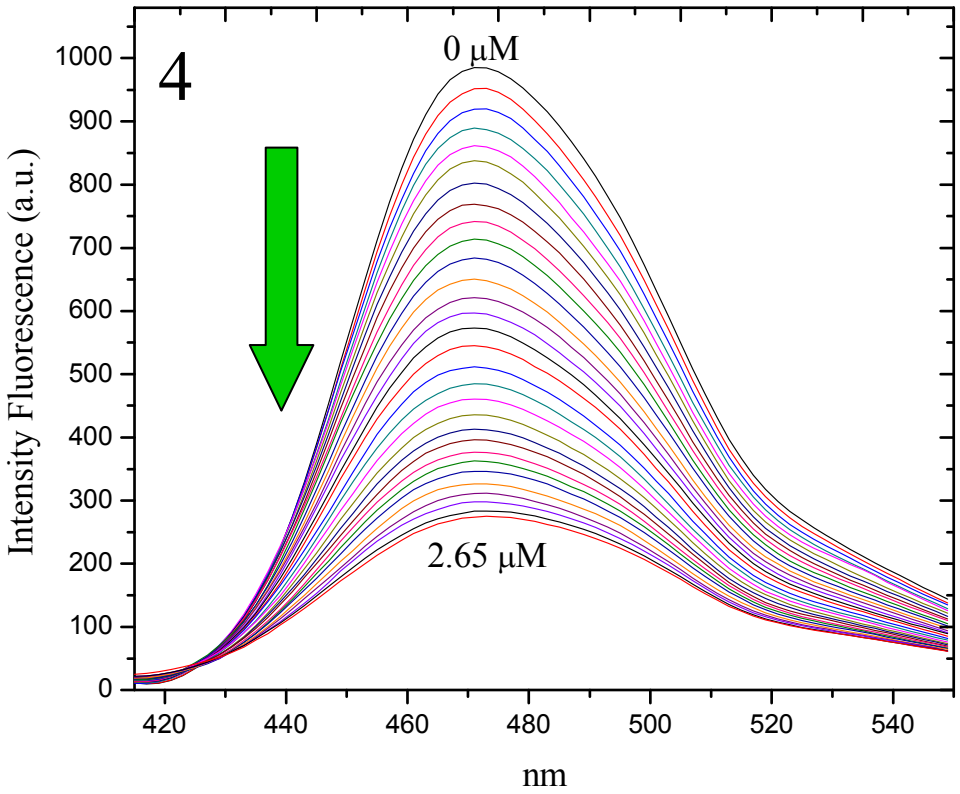

Figure S20. Fluorescence spectra changes of the titration of *h*CaM L39C-*mBBr*/V91C-*mBBr* with tajixanthone hydrate (**4**).

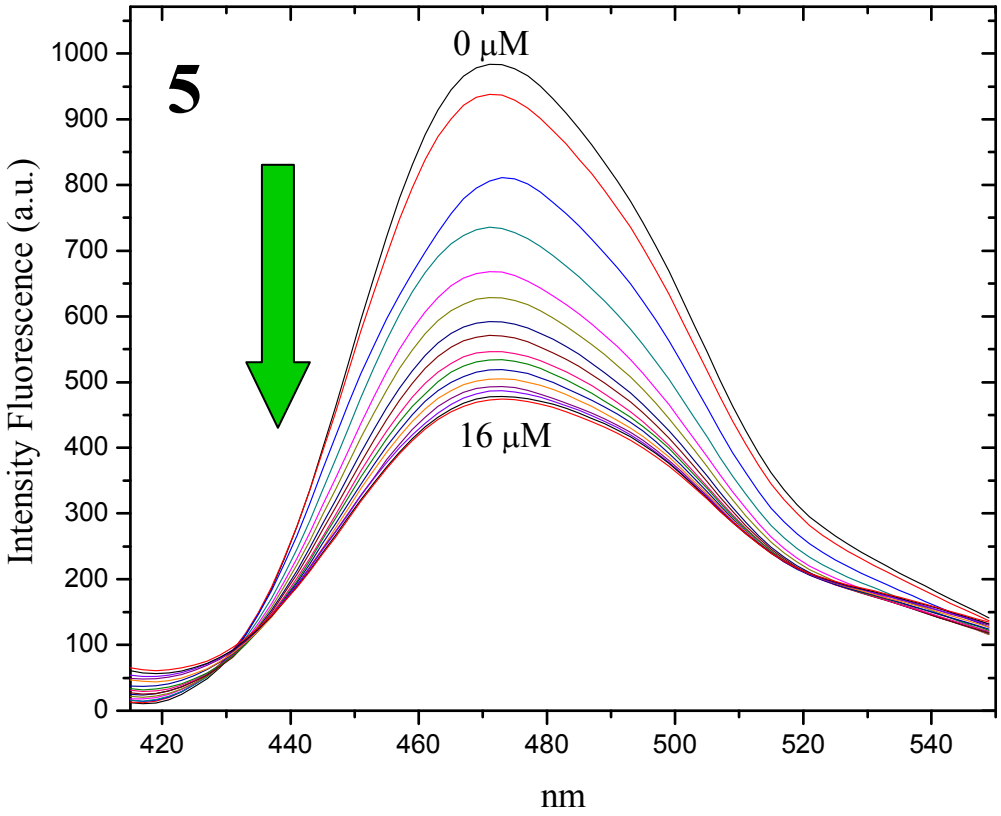

Figure S21. Fluorescence spectra changes of the titration of *h*CaM L39C-*mBBr*/V91C-*mBBr* with 15-acetyl tajixanthone hydrate (**5**).

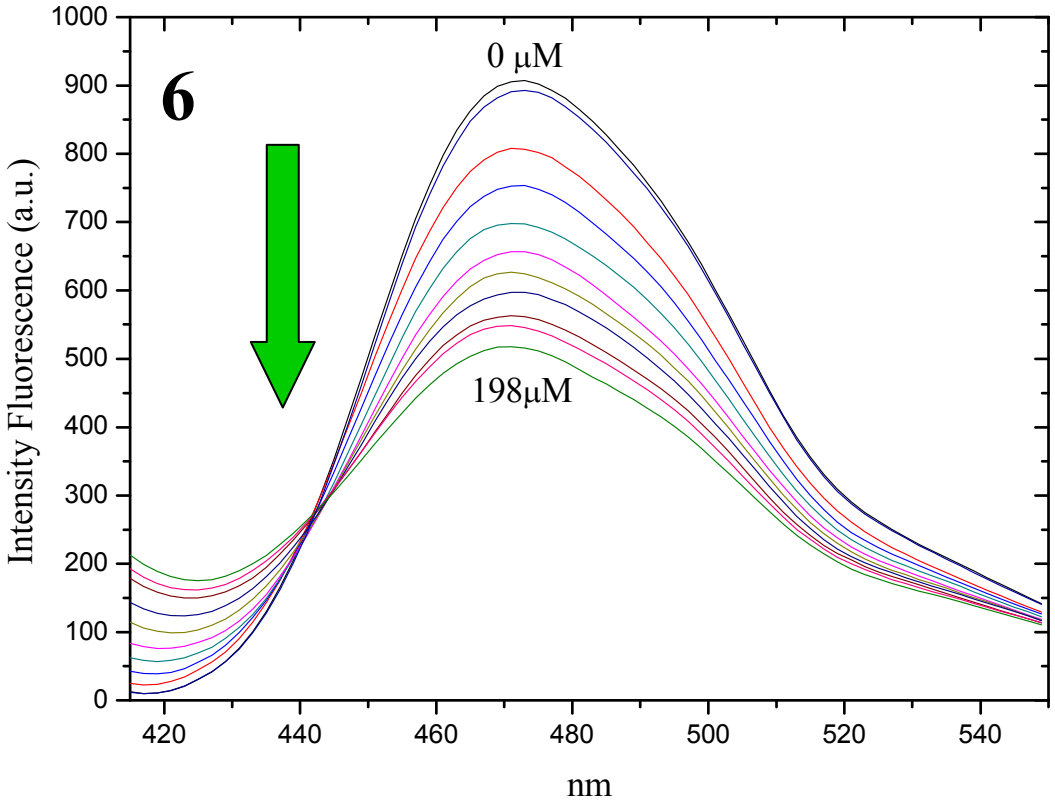

Figure S22. Fluorescence spectra changes of the titration of *h*CaM L39C-*mBBr*/V91C-*mBBr* with 16-chlorotajixanthone (**6**).

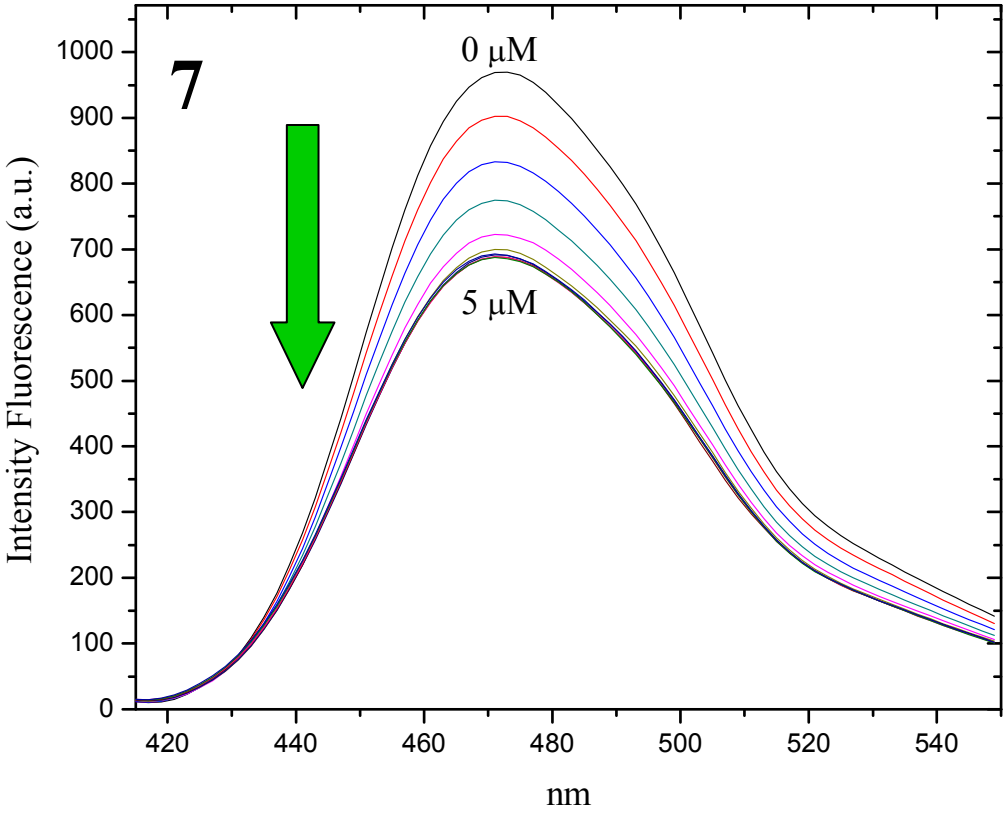

Figure S23. Fluorescence spectra changes of the titration of *h*CaM L39C-*mBBr*/V91C-*mBBr* with emericelline (**7**).

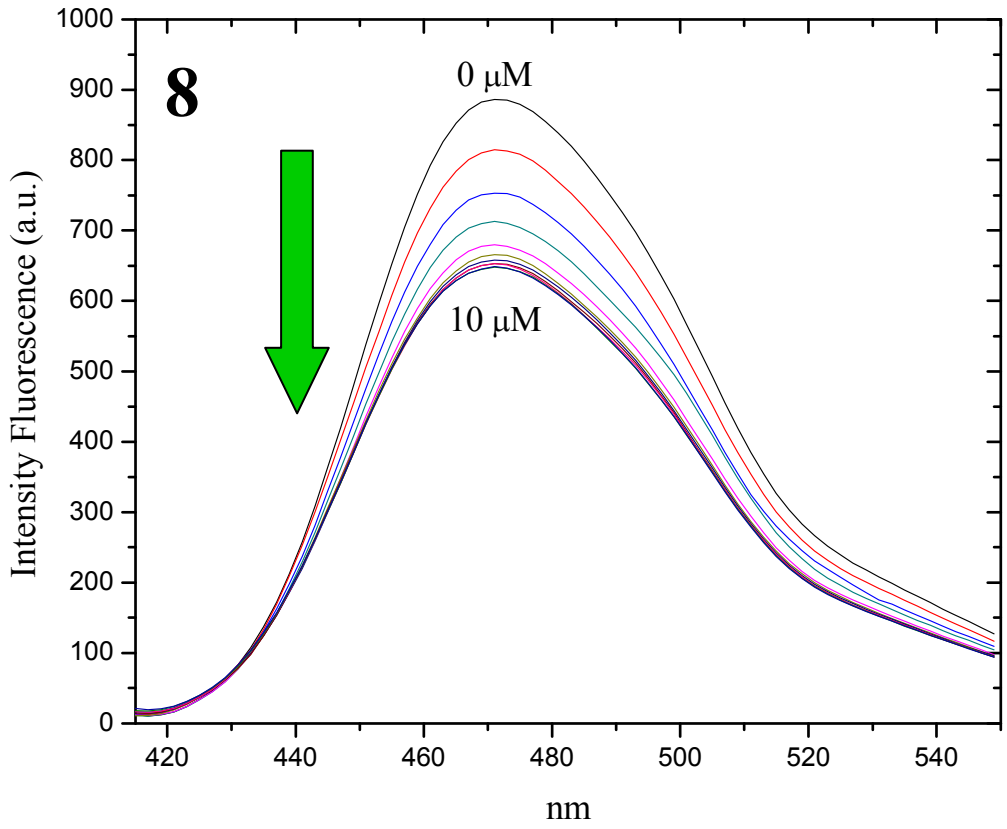

Figure S24. Fluorescence spectra changes of the titration of *h*CaM L39C-*mBBr*/V91C-*mBBr* with variecoxanthone A acetate (**8**).

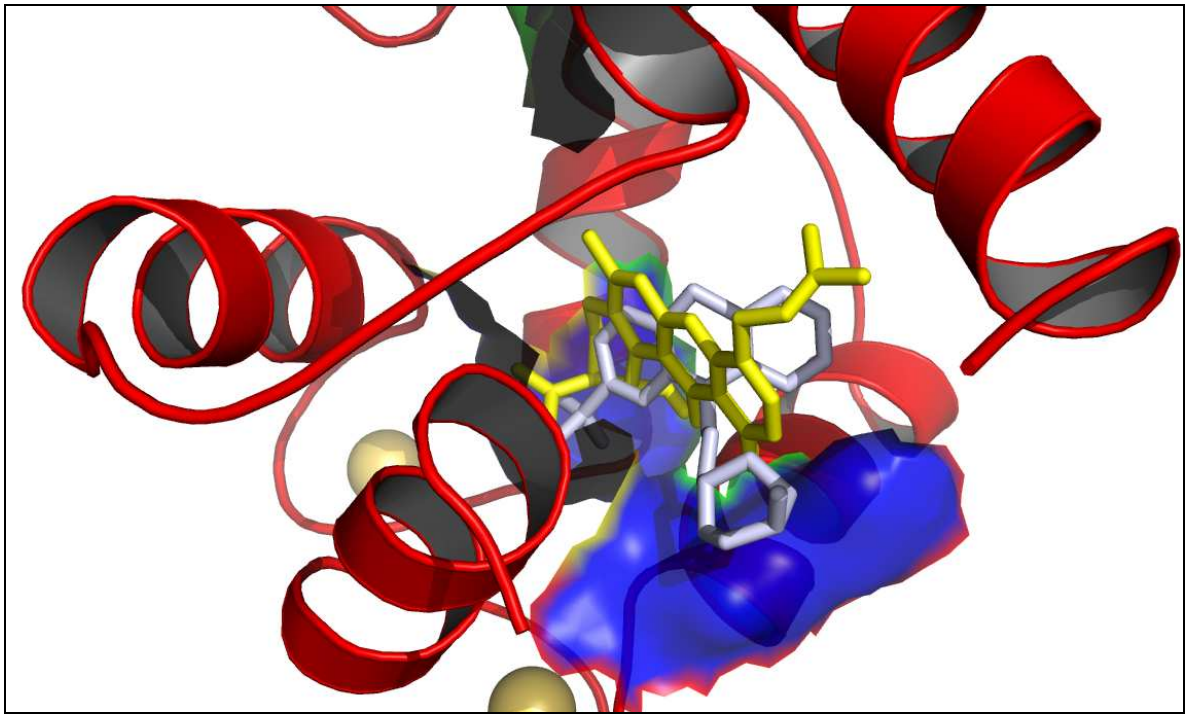

Figure S25. Structural model of Ca^{+2}-CaM-TFP complex represented in red cartoon and the pocket of binding (surface blue) corresponding to sites 1 (Phe92, Ile100, Leu105, Met124, Ile125, Glu127, Ala128, Val136, Phe141 and, Met144), **TFP** depicted in white sticks and compounds **1** is represented in yellow sticks. This figure was geared up using the program PyMOL.

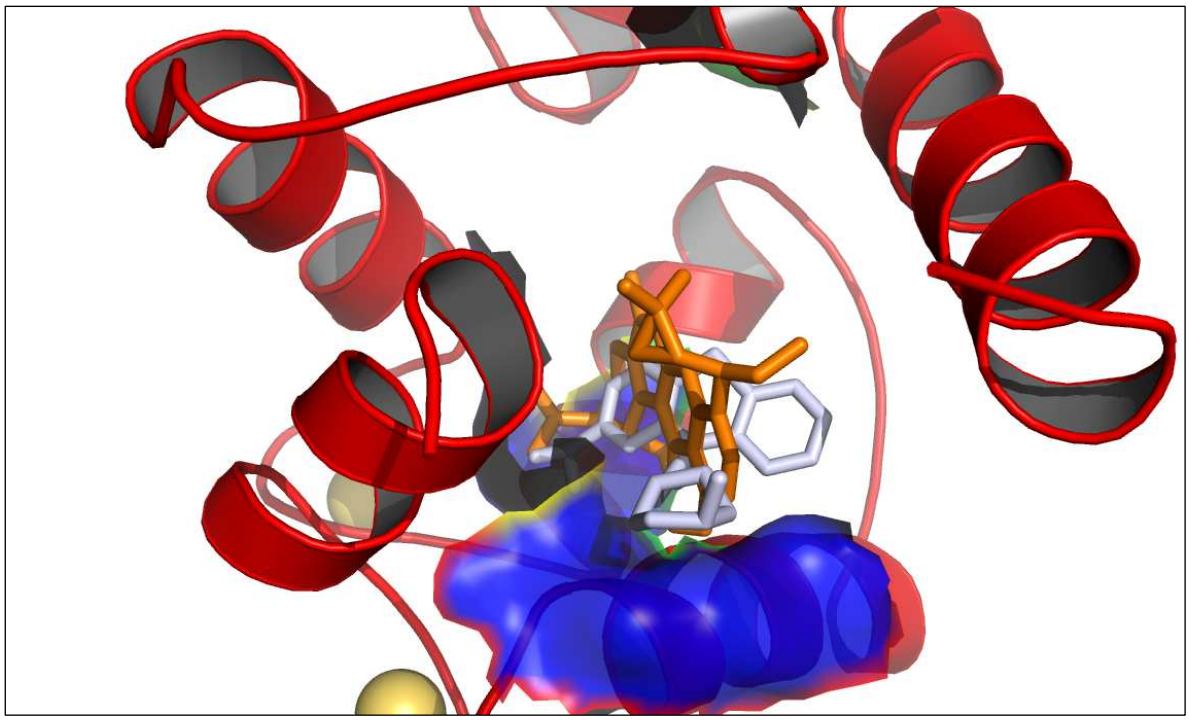

Figure S26. Structural model of Ca^{+2}-CaM-TFP complex represented in red cartoon and the pocket of binding (surface blue) corresponding to sites 1 (Phe92, Ile100, Leu105, Met124, Ile125, Glu127, Ala128, Val136, Phe141 and, Met144), **TFP** depicted in white sticks and compounds **3** is represented in orange sticks. This figure was geared up using the program PyMOL.

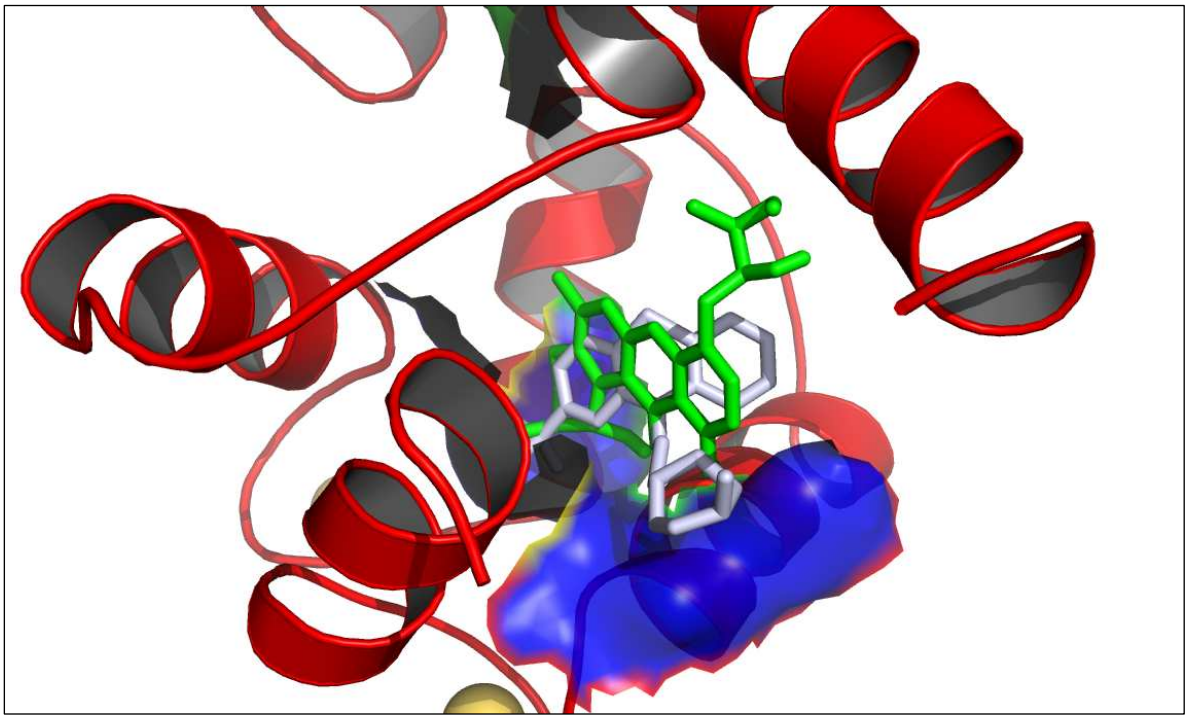

Figure S27. Structural model of Ca^{+2}-CaM-TFP complex represented in red cartoon and the pocket of binding (surface blue) corresponding to sites 1 (Phe92, Ile100, Leu105, Met124, Ile125, Glu127, Ala128, Val136, Phe141 and, Met144), **TFP** depicted in white sticks and compounds **4** is represented in green sticks. This figure was geared up using the program PyMOL.

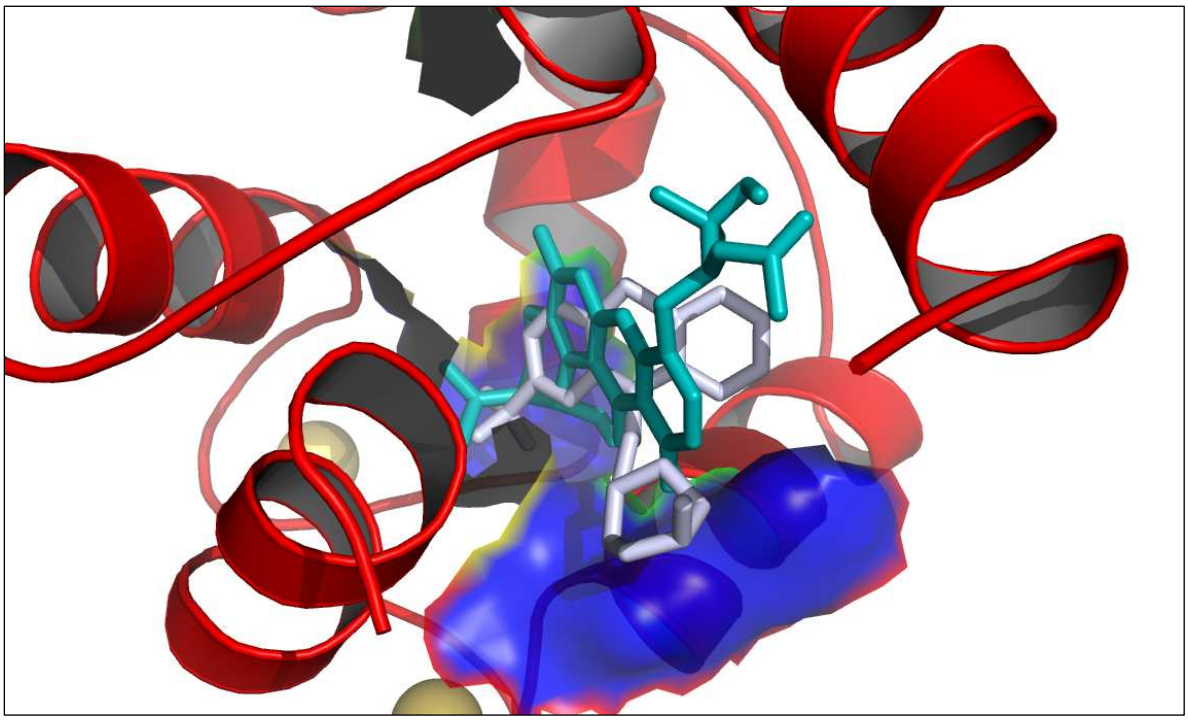

Figure S28. Structural model of Ca^{+2}-CaM-TFP complex represented in red cartoon and the pocket of binding (surface blue) corresponding to sites 1 (Phe92, Ile100, Leu105, Met124, Ile125, Glu127, Ala128, Val136, Phe141 and, Met144), **TFP** depicted in white sticks and compounds **5** is represented in teal sticks. This figure was geared up using the program PyMOL.

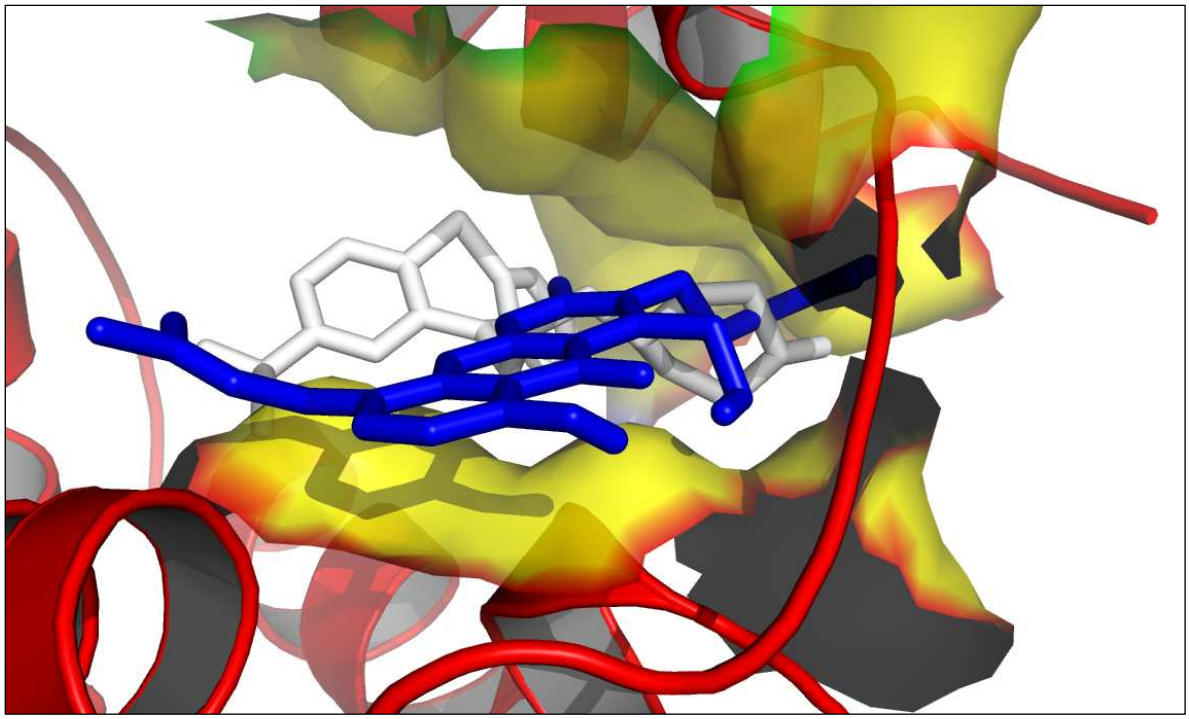

Figure S29. Structural model of Ca^{+2}-CaM-TFP complex represented in red cartoon and the pocket of binding (surface yellow) corresponding to sites 3 (Gln8, Glu11, Phe12, Ala15, Met72, Arg74, Phe92, Met74, Met145 and, Ala147), **TFP** depicted in white sticks and compounds **7** is represented in blue sticks. This figure was geared up using the program PyMOL.

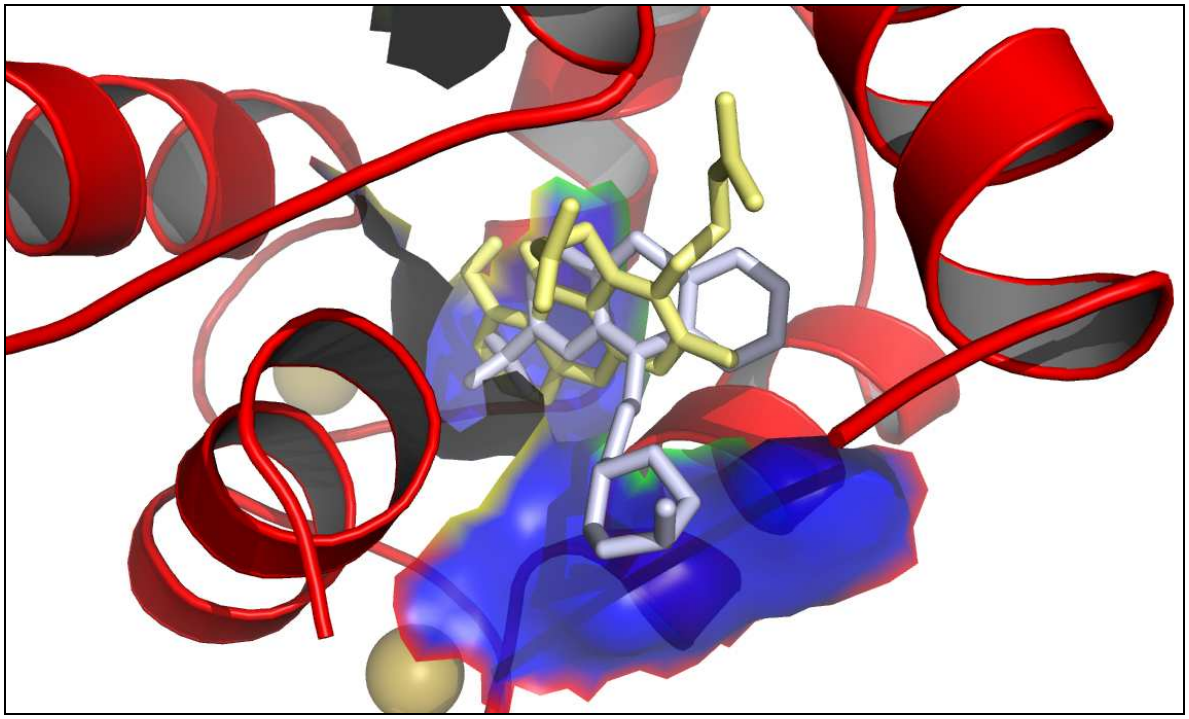

Figure S30. Structural model of Ca^{+2}-CaM-TFP complex represented in red cartoon and the pocket of binding (surface blue) corresponding to sites 1 (Phe92, Ile100, Leu105, Met124, Ile125, Glu127, Ala128, Val136, Phe141 and, Met144), **TFP** depicted in white sticks and compounds **8** is represented in paleyellow sticks. This figure was geared up using the program PyMOL.

Table S1 NMR Data of 15-acetyl tajixanthone hydrate (**5**)

Position	Compound (**5**)		
	δ_C (ppm)	δ_H (ppm), mult (*J* en Hz)	HMBC
1	160.6		H-2, H-3
2	109.6	6.72 *d* (8.0)	H-14a, H-14b
3	137.8	7.42 *d* (8.0)	H-2
4	109.1		H-3, H-14a, H-14b, H-15
5	119.1	7.33 *q* (1.0)	H-24
6	138.5		
7	149.5		H-5, H-19a, H-19b, H-24, H-25
8	121.1		H-24
9	115.1		H-2
10	153.2		H-14a, H-14b, H-15
11	152.0		H-5
12	116.9		H-20, H-25
13	184.1		
14	29.6	a 3.35 *dd* (14.0, 3.0) b 2.90 *dd* (14.2, 10.0)	H-2
15	78.6	5.16 *dd* (10.5, 3.0)	H-14a, H-14b, H-17, H-18
16	72.4		H-14a, H-14b, H-15
17	26.9	1.34 *s*	H-18
18	25.2	1.38 *s*	H-17
19	64.5	a 4.43 *dd* (10.5, 3.2) b 4.35 *dd* (11.0, 3.0)	H-25
20	44.9	2.73 *bs*	H-19a, H-19b, H-22a, H-22b, H-23, H-25, OH-25
21	142.6		H-19a, H-19b, H-25
22	112.2	a 4.22 *s* b 4.57 *s*	H-23
23	22.5	1.85 *s*	H-22a, H-22b
24	17.4	2.36 *d* (1.0)	H-5
25	63.1	5.41 *s*	H-19a, H-19b, OH-25
CH$_3$COO-	20.7	1.87 *s*	
CH$_3$*C*OO-	170.2		*CH*$_3$COO-
OH-1		12.56 *s*	
OH-16		2.37 *s*	
OH-25		4.96 *d* (4.0)	

The ^{13}C Chemical shifts were obtained from ^{13}C-NMR spectra 125 MHz. The ^{1}H Chemical shifts were obtained from ^{1}H-NMR spectra 500 MHz. The correlations reported in these table were obtained from HMBC spectra 500 MHz.

Table S2 NMR Data of 16-chlorotajixanthone (**6**)

Position	Compound (**6**)		
	δ_C (ppm)	δ_H (ppm), mult (*J* en Hz)	HMBC
1	160.5		H-2, H-3
2	110.3	6.80 *d* (8.0)	H-14a, H-14b
3	137.1	7.52 *d* (8.0)	H-2
4	109.3		H-3, H-14a, H-14b, H-15
5	119.3	7.33 *q* (1.0)	H-24
6	138.6		
7	149.6		H-5, H-19a, H-19b, H-24, H-25
8	119.3		H-24
9	115.2		H-2
10	152.1		H-14a, H-14b, H-15
11	152.0		H-5
12	121.1		H-20, H-25
13	184.4		
14	28.6	a 3.05 *d* (8.0) b 3.13 *dd* (16.3, 8.0)	H-2
15	63.4	3.03 *dd* (2.0, 10.5)	H-14a, H-14b, H-17, H-18
16	58.9		H-14a, H-14b, H-15
17	24.8	1.34 *s*	H-18
18	19.0	1.46 *s*	H-17
19	64.6	a 4.44 *dd* (10.8, 3.3) b 4.35 *dd* (11.0, 3.0)	H-25
20	44.9	2.74 *ddd* (3.0, 3.0, 3.5)	H-19a, H-19b, H-22a, H-22b, H-23, H-25, OH-25
21	142.6		H-19a, H-19b, H-25
22	112.3	a 4.82 *dd* (1.5, 2.5) b 4.60 *dd* (1.5, 2.5)	H-23
23	22.5	1.87 *s*	H-22a, H-22b
24	17.4	2.37 *d* (1.0)	H-5
25	63.2	5.43 *ddd* (3.5, 3.0, 1.0)	H-19a, H-19b, OH-25
OH-1		12.66 *s*	
OH-15		2.47 *s*	
OH-25		4.94 *bs*	

The ^{13}C Chemical shifts were obtained from ^{13}C-NMR spectra 125 MHz. The ^{1}H Chemical shifts were obtained from ^{1}H-NMR spectra 500 MHz. The correlations reported in these table were obtained from HMBC spectra 500 MHz.

Table S3 NMR Data of variecoxanthone A acetate (**8**)

Position	Compound (**8**)		
	δ_C (ppm)	δ_H (ppm), mult (*J* in Hz)	HMBC
1	162.0		OH-1, H-2, H-3
2	110.5	6.78 *dd* (8.0, 1.0)	OH-1, H-4
3	136.3	7.57 *t* (8.0)	OH-1
4	106.3	6.88 *dd* (8.0, 1.0)	H-2
5	120.9	7.88 *q* (1.0)	H-19
6	141.6		H-19
7	153.8		H-5, H-14, H-19, H-20
8	117.7		H-5, H-19, H-20
9	109.3		H-2, H-4
10	155.5		H-3, H-4
11	153.9		H-5, H-19
12	128.4		H-5, H-20
13	183.0		OH-1, H-4, H-5
14	71.8	4.39 *d* (7.5)	
15	119.3	5.60 *m*	H-14, H-17, H-18
16	139.1		H-14, H-17, H-18
17	18.0	1.71 *s*	H-18
18	25.8	1.83 *s*	H-17
19	17.5	2.50 *d* (1.0)	H-5
22	58.0	5.79 *s*	
CH$_3$COO-	20.9	2.10 *s*	
CH$_3$*C*OO-	170.9		H-20, H-22
OH-1		12.90 *s*	

The ^{13}C Chemical shifts were obtained from ^{13}C-NMR spectra 125 MHz. The ^{1}H Chemical shifts were obtained from ^{1}H-NMR spectra 500 MHz. The correlations reported in these table were obtained from HMBC spectra 500 MHz.